From the Department of Clinical Science,
Intervention and Technology, Division of Radiology

Karolinska Institutet, Stockholm, Sweden

PERFUSION COMPUTED TOMOGRAPHY OF THE LIVER

Katharina Brehmer

Stockholm 2022

Published by Karolinska Institutet.
Printed by Universitetsservice US-AB, 2022

ISBN 978-91-8016-609-6
Cover illustration: by Katharina Brehmer. Illustration of a hepatocellular carcinoma in liver segment III demonstrated as a time-resolved triple-arterial phase CT, perfusion color maps (ALP, PLP and HPI) and time attenuation curve. Right upper corner shows a coronal time-resolved MIP image for visualization of the arteries in the upper abdomen.

Perfusion Computed Tomography of the Liver

THESIS FOR DOCTORAL DEGREE (Ph.D.)

By

Katharina Brehmer

The thesis will be defended in public at Lecture Hall C1:87, Karolinska University Hospital Huddinge, 20th of May 2022, at 13:00.

Principal Supervisor:
Prof. Torkel Brismar, MD PhD
Karolinska Institutet
Department of Clinical Science,
Intervention and Technology - CLINTEC
Division of Radiology

Co-supervisor(s):
Assoc. Prof. Michael A. Fischer, MD
University of Zurich
Department of Diagnostic and Interventional Radiology

Adjunct Prof. Per Stål, MD PhD
Karolinska Institutet
Department of Medicine, Huddinge
Division of Gastroenterology and Rheumatology

Opponent:
Prof. Wolfgang Schima, MD
Medical University Vienna
Department of Radiology and Nuclear medicine
Division of Radiology

Examination Board:
Assoc.Prof. Maria Kristoffersen-Wiberg, MD PhD
Karolinska Institutet
Department of Clinical Neuroscience
Prof. emerita
Faculty of Medicine and Health Sciences
Department of Diagnostics and
Specialized Medicine
Linköping University

Adjunct Prof. Folke Hammarqvist, MD PhD
Karolinska Institutet
Department of Clinical Science,
Intervention and Technology - CLINTEC
Division of Surgery

Prof. Magnus Båth, MD PhD
Gothenburg University
Department of Clinical Science
Division of Radiophysics

To the two most important persons in my life,

Laura and Pablo.

ABSTRACT

Background: Perfusion CT (P-CT) is a relatively new imaging technique that permits the visual and quantitative assessment of the micro- and macrocirculation of a target organ and focal lesions. P-CT has shown promising results in the evaluation of hyper-vascular tumors such as hepatocellular carcinoma (HCC). HCC is the sixth most common cancer globally and it has a poor prognosis when discovered at a late tumor stage. Any improvement in HCC detection would be directly beneficial for patient care.
This thesis aims to investigate the strengths and limitations of whole liver P-CT and to evaluate if P-CT can improve the detection of hyper-vascular liver lesions in patients with chronic liver disease.
Methods: ***Study I:*** Twenty-four patients, who underwent dynamic P-CT for detection of HCC were retrospectively divided into three groups: (1) without portal-venous hypertension (PVH) (n = 8), (2) with PVH (n = 8), (3) with PVH and thrombosis (n = 8). Time to peak splenic- and peak renal enhancement (PSE resp. PRE), as well as arterial liver perfusion (ALP), portal- venous liver perfusion (PLP) and hepatic perfusion-index (HPI) of the liver and HCC derived from PSE- versus PRE- based modelling were compared between the groups.
Study II: Group A (n=15) and Group B (n= 38) underwent P-CT using 50 ml contrast medium (CM). Group B underwent an additional standard multiphasic liver CT using 120ml (70-143 ml). Triple-arterial CT image sets were reconstructed from P-CT by fusing three dedicated arterial time points. Triple-arterial CT and single-arterial CT were compared by two readers (R1, R2), who assessed subjective image quality (IQ) and HCC detection rate. A third reader assessed objective IQ.
Study III: Fifty study participants (Group A) were scanned with P-CT, a high CM volume protocol and bolus-tracking technique to depict ten arterial phases. Time attenuation curves were created for hyper-vascular liver lesions, liver parenchyma and hepatic vascular structures. 16 participants of Group A with lesions were further analyzed and radiation dose-neutral quadruple arterial phase image sets were created (Group A1). Group A1 was then compared to a Control Group (Group B) consisting of 16 consecutive patients undergoing standard single arterial phase scans. Lesion depiction and quantitative IQ were compared.
Results: ***Study I:*** Time to PSE was significantly delayed in PVH groups 2 and 3 ($P = 0.02$), whereas PRE was similar in groups 1, 2 and 3 ($P > 0.05$). In group 1, liver and HCC perfusion parameters were similar for PSE- and PRE-based modelling (all $P > 0.05$), while significant differences were seen for PLP and HPI (liver only) in group 2 and ALP in group 3 (all $P < 0.05$).
Study II: The mean $CTDI_{vol}$ of triple-arterial CT and single-arterial CT was equivalent ($P=0.73$). Triple-arterial CT showed lower image noise and better contrast-to-noise-ratio ($P<0.001$, $P=0.032$, respectively), but no significant difference in lesion-to-liver-contrast-ratio ($P=0.31$). Subjective IQ was good for both protocols. The detection rate of the 65 HCC lesions was 82%/83% (R1/R2) at triple-arterial CT and 80%/77% (R1/R2) at single-arterial CT ($P=0.4$).
Study III: Both Group A1 and B had 33 hyper-enhancing liver lesions each. The mean $CTDI_{vol}$ of quadruple-arterial CT and single-arterial CT was equivalent ($P=0.16$). The mean time to reach peak lesion-to-liver contrast (LLC) was 20.1s (±4.2s) with a range of 12.5s to 29.1s. Quadruple arterial CT performed significantly better than the Control Group in regards to LLC ($P= .009$), CNR ($P= .002$), Image Noise ($P<0.001$) and hepatic artery enhancement($P<0.001$).
Conclusions: ***Study I:*** PSE is significantly delayed in patients with portal venous hypertension, which results in a miscalculation of P-CT parameters. Maximum-slope based P-CT could be improved by replacing the spleen with the kidney as the reference organ. The difference between time to PSE and time to PRE might serve as a non-invasive biomarker of portal venous hypertension.
Study II: Radiation dose-equivalent triple arterial phase imaging is feasible and showed superior image quality and similar HCC detection rate as standard single arterial phase CT despite a substantially smaller CM volume.
Study III: The optimal scan delay at single arterial phase CT for depiction of hyper-vascular liver lesions occurs at 20 s, when using a high iodine dose CM protocol and bolus-tracking. Fused quadruple arterial phase CT significantly increases lesion depiction, quantitative IQ and hepatic artery enhancement as compared to standard single arterial phase CT, without elevating the total radiation dose.

LIST OF SCIENTIFIC PAPERS

I. Fischer MA, **Brehmer K**, Svensson A, Aspelin P, Brismar TB. **Renal versus splenic maximum slope based perfusion CT modelling in patients with portal-hypertension.** *Eur Radiol*. 2016;26(11):4030-4036. doi:10.1007/s00330-016-4277-7

II. **Brehmer K**, Brismar TB, Morsbach F, Svensson A, Stål P, Tzortzakakis A, Voulgarakis N, Fischer MA. **Triple Arterial Phase CT of the Liver with Radiation Dose Equivalent to That of Single Arterial Phase CT: Initial Experience.** *Radiology*. 2018;289(1):111-118. doi:10.1148/radiol.2018172875

III. **Brehmer K**, Fischer MA, Svensson-Marcial A, Stål P, Brismar TB. **Multiple-arterial phase CT scanning for visualization of focal arterialized liver lesions** *(Manuscript)*

CONTENTS

LIST OF ABBREVIATIONS

AASLD	American Association for the Study of the Liver Diseases
ACR	American College of Radiology
ALP	Arterial liver perfusion
AMS	Adapted maximum-slope method
APHE	Arterial phase hyperenhancement
BCLC	Barcelona-Clínic Liver Cancer
BF	Blood flow
BV	Blood volume
BSC	Best supportive care
CEUS	Contrast enhanced ultrasound
CM	Contrast Material
CNR	Contrast to Noise Ratio
CT	Computed Tomography
$CTDI_{vol}$	CT Dose Index volume
DLP	Dose length product
DNA	Deoxyribonucleic acid
EASL	European Association for the Study of the Liver
HBV	Hepatitis B virus
HCC	Hepatocellular Carcinoma
HCV	Hepatitis C virus
HPI	Hepatic Perfusion Index
HU	Hounsfield units
HVPG	Hepatic venous pressure gradient measurements
IQ	Image Quality
ICC	Intrahepatic cholangiocarcinoma
kV	Kilovolt
LI-RADS	Liver Imaging Reporting and Data System
LLC	lesion-to-liver contrast
mAs	milliampere-seconds
MRI	Magnetic resonance imaging
MTT	Mean transit time
mGy	Milligrey

mL	Milliliter
mSv	Millisievert
NAFLD	Non-alcoholic fatty liver disease
PACS	Picture archiving and communication system
P-CT	Perfusion CT
PLP or PVP	Portal-venous liver perfusion
PRE	Peak renal enhancement
PSE	Peak splenic enhancement
PS	Permeability surface-area product
PVH	Portal venous hypertension
RECIST	Response Evaluation Criteria In Solid Tumors
ROI	Region of interest
s	Second
SNR	Signal-to-noise-ratio
TAC	Time attenuation curve
TACE	Trans-arterial chemoembolization
TTP	Time to peak enhancement
TLP	Total liver perfusion
US	Ultrasound

1 INTRODUCTION AND BACKGROUND

1.1 LIVER ANATOMY

The liver is the largest visceral organ and is positioned in the right upper quadrant of the peritoneal cavity[1,2]. The liver is divided into two lobes and subdivided into 8 anatomical segments according to the classification by Couinaud[1]. It has many important functions such as bile production and excretion, metabolism of drugs and toxins, storage of glycogen, vitamins and minerals, excretion of cholesterol, hormones and bilirubin, production of clotting factors and other plasma proteins. The liver is also involved in the metabolism of fats, proteins and carbohydrates as well as in the activation of certain enzymes.

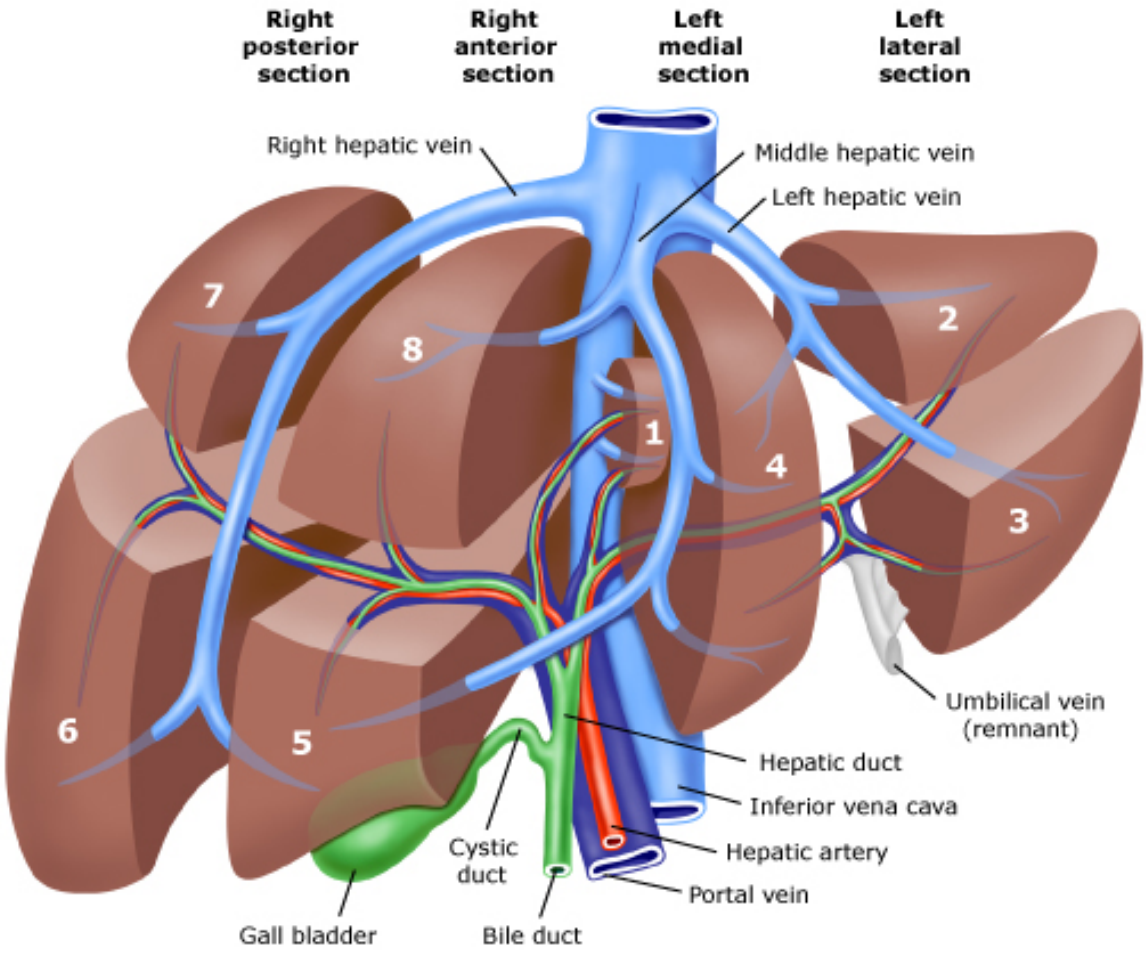

Figure 1. Illustration of anatomic segmentation and dual blood supply of the liver (©[3])

For contrast enhanced imaging of the liver it is essential to understand its unique dual blood supply (Figure 1). The organ receives oxygenated blood from the hepatic artery and partly deoxygenated nutrient-rich blood from the portal vein. The hepatic arterial branches commonly arise from the common hepatic artery which usually originates from the celiac trunc and they account for approximately 25 % of the livers blood supply. The main blood supply (approximately 75 %) is provided by the portal vein, which delivers blood from the

intestines and the spleen. The smallest structural and functional compartments in the liver are called lobules. In each lobule there is a central vein, which drains into collecting veins which in turn drain into hepatic veins and further on into the inferior vena cava[3].

1.2 LIVER CIRRHOSIS

Cirrhosis is a progressive disease characterized by architectural changes in the liver parenchyma that directly affect the micro- and microcirculation of the liver. Capillaries with a continuous vascular wall replace the normal wide-fenestrated sinusoids and there is an increasing deposition of collagen in the perisinusoidal space of Disse. These changes lead to increased vascular resistance and consequently reduced portal venous blood flow. As the portal venous blood flow decreases the hepatic arterial blood flow increases. This phenomenon is called the hepatic arterial buffer response[4]. In the newly formed continuous capillaries the exchange of big molecules from the intravascular space to the extravascular space of Disse is restricted[5,6].
The main causes for cirrhosis are chronic hepatitis B (HBV), C (HCV) and D virus infections, alcohol overconsumption, and non-alcoholic fatty liver disease (NAFLD) related to obesity, Type 2 diabetes and the metabolic syndrome. Risk factors differ widely depending on geographic region and they have started to shift due to the more widespread use of antiviral therapies and vaccination programs against hepatitis B virus on one hand, and the rise of excess body weight and diabetes on the other hand[7].

1.3 HEPATOCELLULAR CARCINOMA – EPIDEMIOLOGY

According to the GLOBOCAN Report of 2020 “Primary liver cancer is the sixth most commonly diagnosed cancer and the third leading cause of cancer death worldwide in 2020, with approximately 906,000 new cases and 830,000 deaths.”[7]. In men, both its incidence and mortality are two- to threefold higher than in women. Thus, liver cancer ranks on fifth place in global cancer incidence and on second place in cancer related death in men[7].

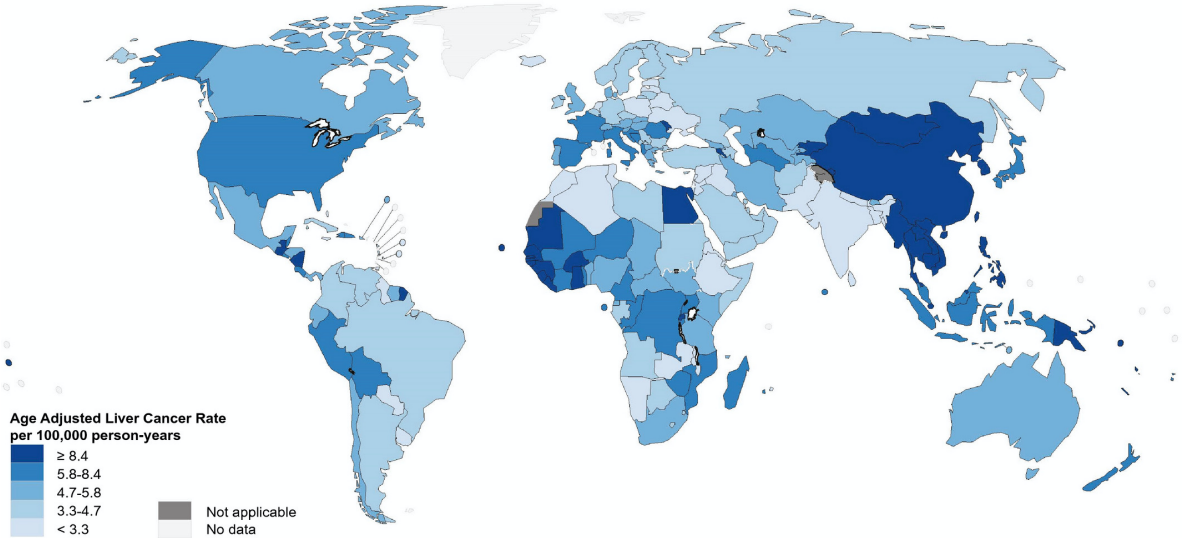

Figure 2. Global age-adjusted incidence rates of liver cancer, estimated for 2018. Data source: GLOBOCAN 2018. Graph production: IARC (http://gco.iarc.fr/today), World Health Organization[8].

The most common type of primary liver cancer is hepatocellular carcinoma (HCC), which constitutes 75%-85 % of all cases[8] . Intrahepatic cholangiocarcinoma (ICC) accounts for 10%-15% and other types of primary liver cancer such as combined HCC-ICC are very rare[9]. In this thesis, special focus was put on HCC as it is the most common liver cancer and is (usually) a highly vascularized tumor and therefore very suitable for perfusion CT (P-CT) imaging[10-14].

Since HCC is predominantly found in chronic liver disease (90%)[15], the main risk factors for HCC are the same as mentioned above for the development of cirrhosis and, in addition, exposure to aflatoxin B1-contaminated foods. Overall, one-third of patients with cirrhosis will develop HCC during their lifetime[16]. Aflatoxin-contaminated foods are known to be hepatocarcinogenic and their cancerogenic effect has been found to increase four- to twelve-fold in combination with chronic HBV infection[17]. This synergistic effect of chronic HBV infection and aflatoxin B1 exposure causes very high HCC incidence rates in East Asia and sub-Saharan Africa. It also explains the considerably earlier onset of HCC in these populations than compared to populations exposed to other risk factors[8]. HBV is the most prominent risk factor globally causing approximately 50 % of all HCC[16]. HBV is a DNA virus that can integrate into the host genome causing mutations and oncogene activation. HBV increases the risk of HCC even in the absence of cirrhosis, but the majority of patients with HBV-induced HCC have cirrhosis at presentation[15]. Depending on the geographical region, approximately 15–30% of HCC cases are caused by alcohol-related cirrhosis[15]. In western countries, NAFLD, which is associated with obesity, diabetes mellitus and the metabolic syndrome, is the fastest growing cause of HCC[15]. HCV infection is still the main cause for HCC in Europe, Japan and North America, but there is a clear positive trend with the successful introduction of antiviral therapies causing so-called sustained virological response[15]. The sustained virological response results in a 50-80% decrease in the risk of developing HCC. However, patients with cirrhosis are still at high risk to develop HCC even after the elimination of HCV and have to continue with their surveillance protocol[15].

Analyzing the described risk factors for HCC, it is clear that most cases can be prevented through vaccination against HBV, antiviral treatment, safe injection practices and safe blood transfusions, as well as interventions to reduce excessive alcohol use and obesity[18].

The prognosis of a patient with HCC worsens drastically with increasing tumor stage. There are several different staging systems, of which the Barcelona-Clínic Liver Cancer (BCLC) staging system[19-21] is the most validated. It has been endorsed by both the American Association for the Study of the Liver Diseases (AASLD) and the European Association for the Study of the Liver (EASL) since it has been shown to offer the most prognostic information[16,22](Figure 3).

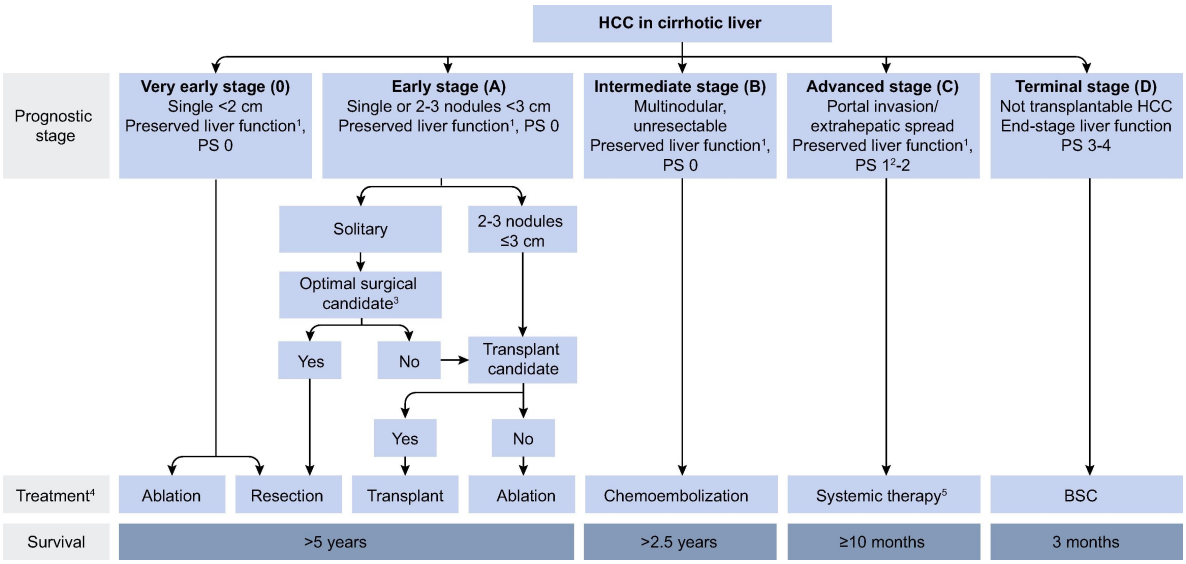

Figure 3. Modified BCLC staging system and treatment strategy with permission to reprint from EASL Clinical Practice Guidelines[16]. PS = performance status; BSC = best supportive care.

The BCLC staging system takes not only into account how localized or widespread HCC is but also considers the patients` performance status and whether the liver function is preserved or not. Only patients in the two earliest stages, Stage 0 and A, are eligible for curative treatment and, therefore, the mean survival is significantly better for these patients than for patients with more advanced stages. For early-stage HCC with curative options the 5-year survival exceeds 70%, whereas patients with symptomatic advanced-stage HCC have a median survival of around 1-1.5 years when treated with systemic therapies and of approximately 8 months without systemic treatment[15].
There are three different types of curative treatment: surgical resection, ablation and liver transplantation. Because of the high mortality of HCC and the clearly better prognosis when detected early, AASLD and EASL recommend surveillance for patients with compensated cirrhosis[15].

1.4 COMMON LIVER IMAGING MODALITIES FOR HCC

Surveillance:
AASLD and EASL guidelines recommend surveillance with ultrasound (US) (with or without the blood biomarker α-fetoprotein) every six months in patients with Child-Pugh A-B cirrhosis, certain subgroups of patients with HBV without cirrhosis and patients on the liver transplantation waiting list[16,22]. The diagnostic accuracy of ultrasound is acceptable when used as a surveillance test (sensitivity ranging from 58 to 89%; specificity greater than 90%)[16,23]. However, ultrasound performs less well for detection of early-stage HCC, with a sensitivity of only 63%[15,16,22]. Screening with cross-sectional imaging modalities Computed Tomography (CT) and Magnetic resonance imaging (MRI) would considerably increase the detection rate but is so far not feasible, because of several associated

disadvantages such as low cost-effectiveness, radiation and contrast material (CM) exposure as well as radiological backlog[22].

Imaging-based diagnosis of HCC:

Dynamic contrast enhanced imaging plays the main role in the diagnosis of HCC in the setting of cirrhosis ever since the diagnostic accuracy of the typical radiological hallmarks of HCC was demonstrated and approved two decades ago[24]. The typical hallmarks of HCC, according to the EASL guidelines, consist of the combination of hypervascularity in the late arterial phase and wash-out appearance on portal-venous and/or delayed phase[16]. The American College of Radiology (ACR) and AASLD support the Liver Imaging Reporting and Data System (LI-RADS), which provides standardization for HCC imaging in the contexts of surveillance, diagnosis, and treatment response assessment[25]. LI-RADS is a diagnosis decision tool that helps categorize lesions into eight subcategories to stratify the probability of HCC and overall malignancy[25] (Figure 4). LI-RADS considers not only the two above mentioned imaging hallmarks, but also includes two additional major features in their diagnostic assessment: the presence or absence of an enhancing "capsule" and threshold growth. In LI-RADS, late arterial phase hyperenhancement (APHE)[25].

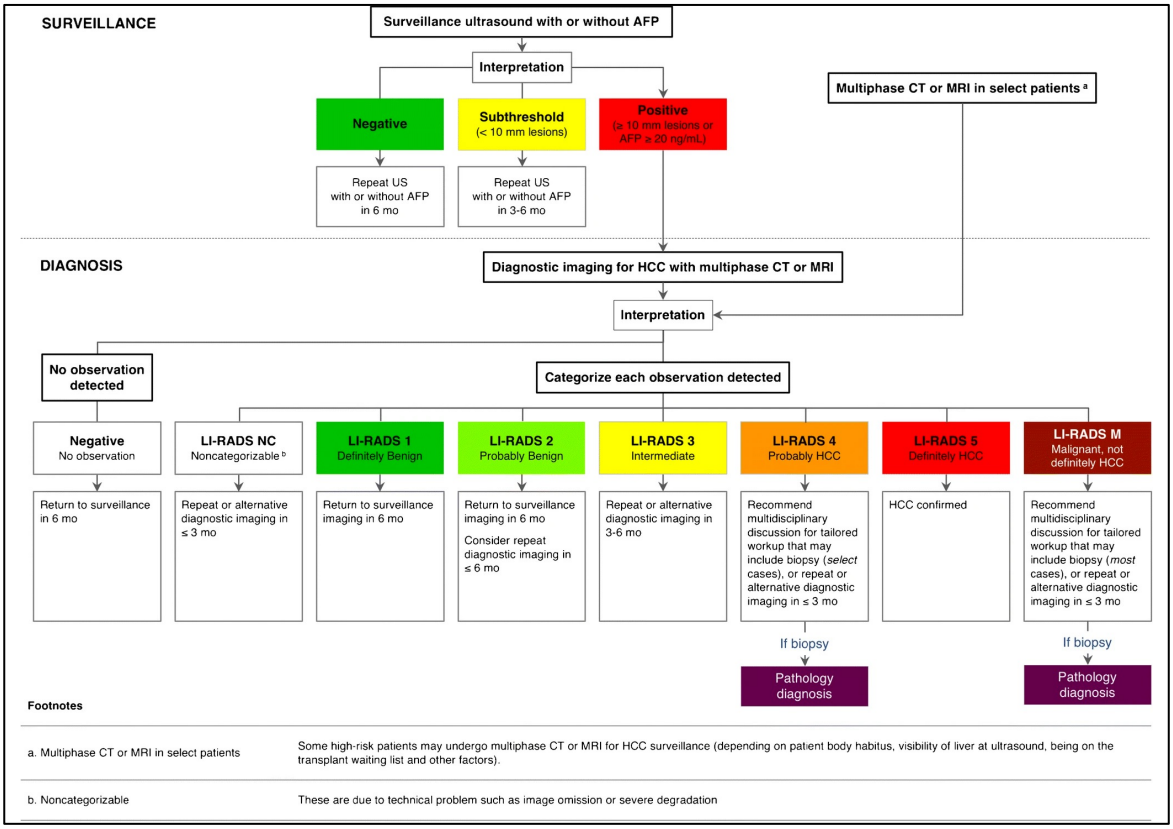

Figure 4. LI-RADS management algorithm. Reprinted with permission from Springer Nature[26].

Performance of CT and MRI for diagnosis of HCC:

The reported sensitivity and specificity of CT and MRI in the literature show a wide range[16]. A systematic review and meta-analysis from 2015 showed comparable sensitivities of MRI and CT for HCC diagnosis on a per-patient basis (88% vs 74%–100%) and comparable specificity of MRI and CT (94% vs 81%–100%)[27]. On a per-lesion basis, the overall sensitivity of MRI was higher than that of CT (79% vs 72%)[27]. Summarized per-lesion sensitivity was significantly lower for HCCs smaller than 1 cm than for larger HCCs (P< .001 for CT, P = .02 for MRI)[27]. Gadoxetic acid–enhanced MRI showed significantly higher per-lesion sensitivity than MRI performed with extracellular contrast agents (87% vs 74%, P = .03)[27]. In summary, MRI shows a slightly higher sensitivity rate than CT and both modalities perform considerably worse in smaller lesions (< 2 cm)[16,28-30]. The use of hepatobiliary MRI contrast agents is recommended, due to higher sensitivity, especially in small HCC [16].

Contrast Enhanced Ultrasound (CEUS):

The enhancement pattern of HCC on CEUS differs slightly from the enhancement pattern seen on CT or MRI. This can be explained by the fact that the contrast agents used for CEUS are intravascular agents while iodine- and gadolinium-based contrast agents are extracellular [16]. In contrary to those at CT and MRI, the arterial enhancement and washout on CEUS are not specific for HCC but are also common in cholangiocarcinoma. This made it necessary to the refine the diagnostic HCC imaging criteria at CEUS. To be diagnostic HCC must have arterial enhancement and *late* washout (>60 s) of mild degree. Cholangiocarcinoma, on the other hand, shows an *earlier* washout (<60 s) and with more marked intensity[16]. The strengths of CEUS when using these refined HCC hallmarks are a very high positive predictive value for HCC of almost 99% and also high specificity of 93% (vs. 77% for CT and 83% for MRI, respectively)[16]. On the other hand, CEUS` sensitivity is significantly lower than for either CT or MRI. It is reported that around 13% of HCC detected on CT or MRI were missed by CEUS[16]. Reasons for that are a relatively short arterial phase on CEUS that does not allow a thorough scan of the whole liver and, additionally, certain areas of the liver that might be difficult to visualize. In summary, CEUS can be used to characterize one or few lesions detected on baseline US, or as a second-line imaging technique when CT or MRI are inconclusive or contraindicated. CEUS is not recommended as a first-line imaging technique to characterize lesions depicted during surveillance, since it is not a suitable technique for tumor staging. In clinical practice, CT or MRI is used for staging[16].

In the non-cirrhotic liver it is not possible to make the diagnosis of HCC based on imaging only. This is because the imaging hallmarks of HCC in the non-cirrhotic liver are less specific due to a higher prevalence of alternative diagnoses [16]. To make the diagnosis of HCC in the normal liver it is necessary to take a biopsy.

1.5 PRINCIPLES OF PERFUSION IMAGING

Perfusion is defined as the transport of blood to a unit volume of tissue. Liver perfusion can be evaluated with CT when specific fast dynamic scan techniques are applied[31]: The liver is scanned multiple times with short (1.5 – 4 seconds) intervals before, during and after simultaneous CM administration. Changes in tissue CT attenuation over time are directly proportional to the local iodine concentration within the microvasculature and interstitial space of the examined tissue[31]. P-CT can therefore provide functional information about the microcirculation of the liver parenchyma and of focal liver lesions[10,32-35].
For P-CT imaging, it is necessary to understand the specific pharmacokinetics of iodine based CM, which can be divided into two phases: the first pass ("perfusion phase") and the delayed phase ("interstitial phase"). During the first phase, which lasts for around 40 – 60 seconds, iodine is mainly contained in the intravascular compartment. During this phase, perfusion measurements such as tissue blood flow (BF) and time to peak enhancement (TTP) can be evaluated. During the delayed phase, contrast medium passes across the capillary basement membrane, from the intravascular space into the extravascular extracellular space. By quantifying the amount of iodine in the intravascular and the extravascular space it is possible to measure the vascular permeability. The delayed phase ranges from 2-10 minutes after contrast injection[10,11,33,35-38].

Different kinetic models:
A range of mathematical models can be used to quantify tissue perfusion and/or permeability from the volume P-CT raw data[34,36,39-41]. The kinetic method called "dual maximum slope method" is the most commonly used model for liver perfusion quantification since this method is less complicated and more robust than other models[34,38]. The method has been proposed by Blomley et al[34] and modified by Tsushima et al[42] for voxel-based imaging. The time of maximum enhancement in the spleen is used to separate arterial and portal-venous liver enhancement. Then the maximum slope of each voxel time attenuation curve is calculated separately before and after this peak splenic separation time point and divided by the peak arterial and peak portal venous enhancement respectively (Figure 5).

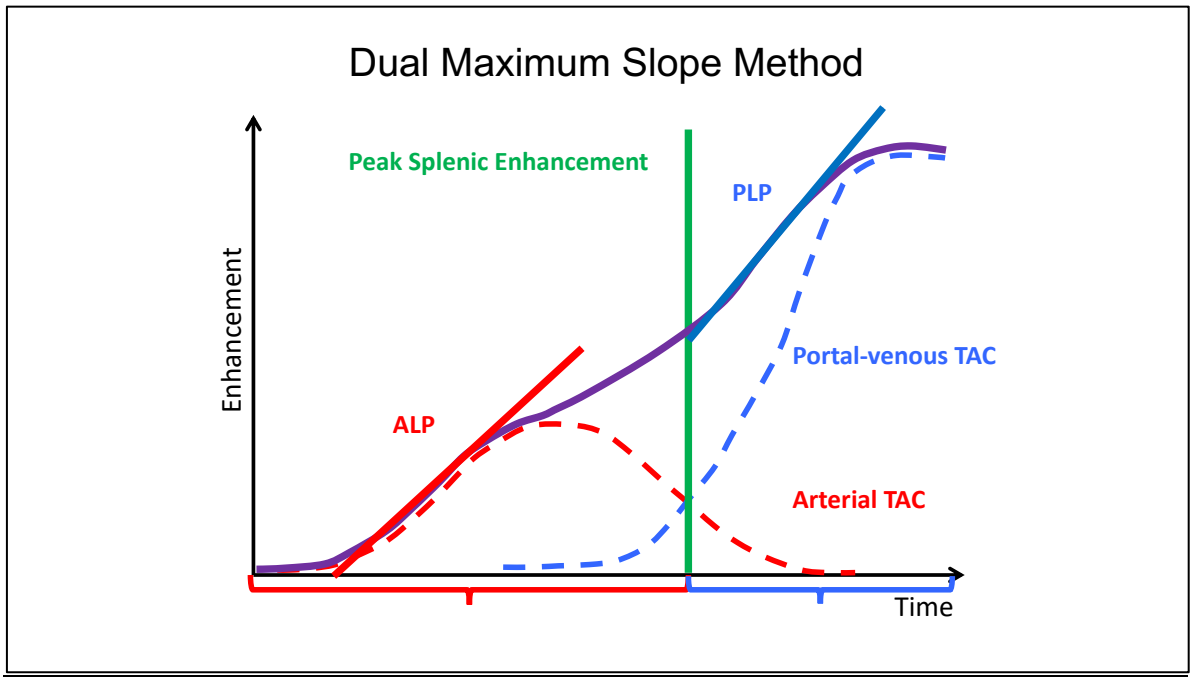

Figure 5. Schematic illustration of liver perfusion (purple curve) calculated with the dual maximum slope method to separate arterial liver perfusion (red line) and portal-venous liver perfusion (blue line). Time to peak splenic enhancement is commonly used as a separation point in commercially available CT body perfusion software. ALP = arterial liver perfusion, PLP = portal-venous liver perfusion, TAC = time attenuation curve.

However, the maximum slope method allows only for the calculation of perfusion parameters of the first pass-phase; i.e. arterial, portal venous and total liver perfusion (TLP), hepatic perfusion index (HPI) and time to peak enhancement (TTP). HPI is defined as the proportion of arterial liver perfusion of the total liver perfusion[32,38].
Other common kinetic models are the Patlak model and the Johnson-Wilson method, with which perfusion values such as blood volume (BV), mean transit time (MTT) and permeability surface-area product (PS) can be derived. A variety of different kinetic models are described in more detail in the literature[34,36,39-41].

1.6 LIVER PERFUSION CT ACQUISITION AND POST-PROCESSING TECHNIQUE

Liver P-CT acquisition:
Different liver P-CT protocols have been described in the literature. The main elements of all P-CT protocols are a non-enhanced baseline scan and fast sequential scanning during and after CM injection. Perfusion protocols can differ in several parameters such as image cycle time, total acquisition time (only first pass- and/or delayed phase acquisition), tube voltage- and tube current-settings, scan length in z-axis, scan technique (wide detector, shuttle/jog mode, continuous spiral mode) and CM administration protocol. The choice of CT protocol depends mainly on which perfusion parameters one wants to assess and, therefore, if the first pass and/or the delayed phase should be depicted. Furthermore, the

choice of protocol depends on the type and vendor of the CT scanner, on the type of kinetic model used and which software solution is available[33,35,43-45].
For the CM injection a short and well-defined bolus (40-70 ml CM volume) and a high injection flow rate (4-10 ml/sec) are necessary to guarantee correct perfusion measurements[11,45]. Contrast medium with an iodine concentration of >300 mg/mL are recommended to obtain sufficiently high contrast-to-noise ratios (CNR)[32].

Image Post-Processing:
In liver P-CT imaging, post-processing steps to correct motion artefacts and image noise are essential to enhance image quality. Since the liver is scanned multiple times (often up to 30 times), each split series is performed with as low radiation dose as possible, which results in low quality raw data images. Motion artefacts are also a big concern in P-CT imaging as patients usually cannot hold their breath during the whole duration of the total acquisition time of about 40-50 s. Fortunately, there are very good software options available to significantly reduce both image noise and motion artefacts. In our studies, we have applied automated motion correction and noise reduction using a non-rigid deformable registration technique as described by Wang et al[46].
This method allows for motion correction and correction of soft-tissue deformation caused by breathing artefacts. After these two automated correction steps have been performed, multiple split series of a volume P-CT scan can be matched and averaged on a voxel-by-voxel basis to generate a fused or time-resolved image with greatly improved soft-tissue contrast and reduced random noise[46]. CT image noise due to low tube current usually follows a random distribution, and by combining several images random noise can be reduced. The increase in image quality improves incrementally dependent on the number of split series used. When co-registering 10 split series, this procedure enhances the signal-to-noise-ratio (SNR) by a mean factor of 3 over the original image quality[46].
These described post-processing steps of automated motion correction and noise reduction should be applied to enhance image quality both when color coded perfusion maps are created and as well when averaging several split series as we have done in Study II and III.

1.7 PERFUSION DATA ANALYSIS

The acquired volume perfusion dataset contains both morphological and functional information, that can be evaluated both visually and quantitatively[32,35]:
Qualitative or visual analysis can be performed by visual assessment of so-called time attenuation curves (TAC) (Figure 6), color coded perfusion maps (Figure 8) and of reconstructed time-resolved image sets (Figure 7). TAC show attenuation changes over time in a specified region of interest (ROI) and can be visually analyzed in regards to their shape (e.g. enhancement slope; whether there is wash-out or a plateau). Moreover, morphologic image sets can be reconstructed by fusion of several split series, simulating

the different phases of a standard multi-phasic liver CT (Figure 7). This allows for a standard radiological evaluation of the enhancement pattern of focal liver lesions.

Figure 6. Time attenuation curves (yellow lines) and quantitative perfusion parameters (grey boxes) of non-tumorous liver parenchyma (a) and hepatocellular carcinoma (b) (BV: blood volume, MTT: mean transit time, ALP: arterial liver perfusion, PVP: portal-venous liver perfusion and HPI: hepatic perfusion index). With permission to reprint from Elsevier B.V., Kartalis et al.[31]

Figure 7. Images of a patient with liver cirrhosis and a hepatocellular carcinoma in the left lateral liver segment (arrow). The fusion of three split series acquired at 8 s (a), 13 s (b) and 24 s (c) result in the axial time-resolved image (d) and the coronal maximum intensity projection (e), where the vascular anatomy is nicely demonstrated. With permission to reprint from Elsevier B.V., Kartalis et al.[31]

Furthermore, *quantitative* analysis of TAC permits the measurement of peak enhancement times and peak enhancement values of all structures captured in the volume P-CT scan. At last, *quantitative* analysis of tissue perfusion is possible by applying kinetic models and calculating perfusion parameters as described before. Perfusion parameters can also be displayed in quantitative color coded maps which can aid in the detection of focal liver lesions (Figure 8)[35].

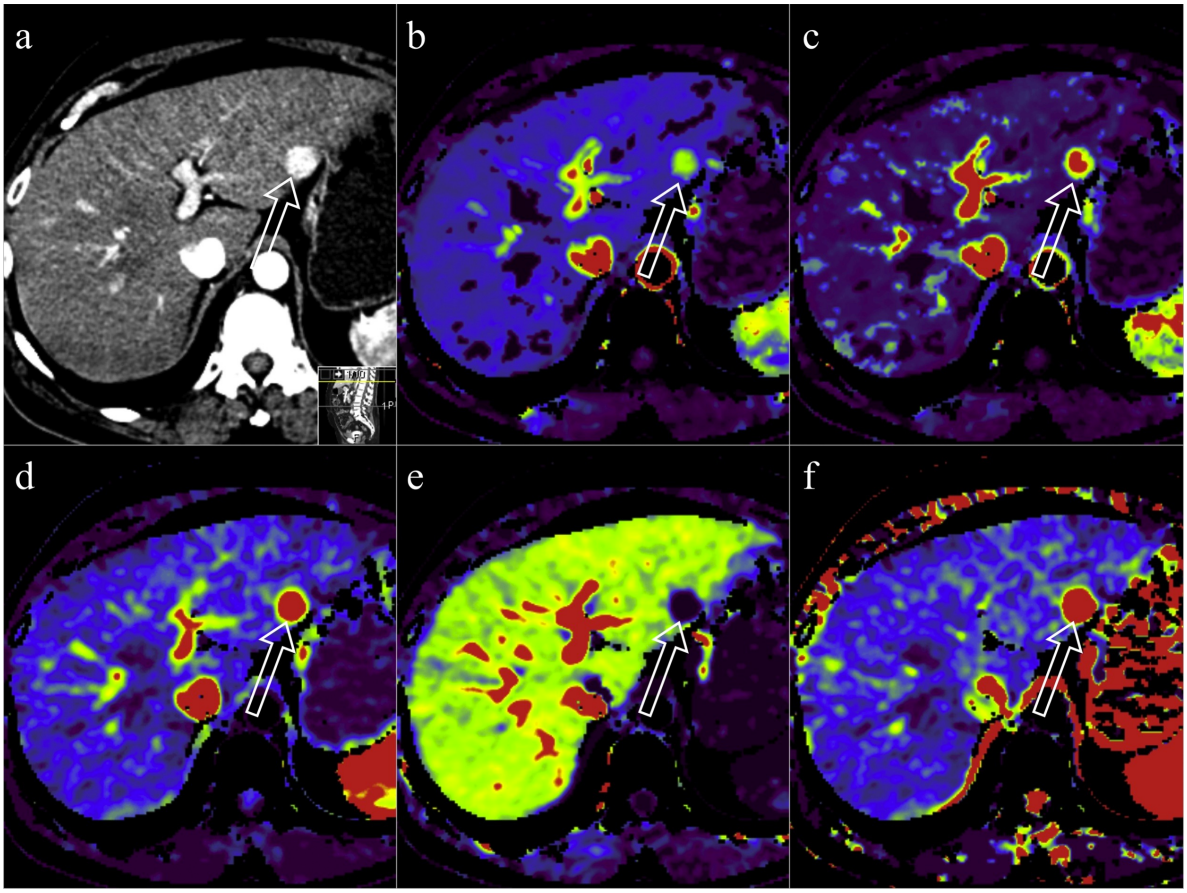

Figure 8. *Perfusion CT of a patient with liver cirrhosis and a hepatocellular carcinoma (arrow) in the left lateral liver segment. Image (a) represents a time-resolved maximum intensity projection and (b–f) are colour-coded maps of the following perfusion parameters: blood flow (b), blood volume (c), arterial liver perfusion (d), portal-venous liver perfusion (e) and hepatic perfusion index (f). With permission to reprint from Elsevier B.V., Kartalis et al.* [31]

<u>Perfusion parameters:</u>

Different perfusion parameters can be calculated depending on which scan protocol was performed and which mathematic model was used. The most common perfusion parameters are described in Table 1[10,33,35].

Perfusion Parameter	Definition	Unit	Property
Tissue blood flow (BF)	Volume flow rate of blood through the vasculature	mL/min/100g of tissue	Perfusion; vascular density
Tissue blood volume (BV)	Volume of moving blood within the vasculature of a tissue region	mL/100g of tissue	Vascular density
Mean transit time (MTT)	Average time for the blood to pass through the capillary network	seconds	Measure of tumor interstitial pressure and vessel leakiness
Permeability surface-area product (PS)	Unidirectional diffusional flux from blood to interstitial space per unit capillary surface area	mL/min/100g of tissue	Capillary leakage
Arterial liver perfusion (ALP)	Arterial liver blood flow	mL/min/100g of tissue	Detection of predominantly arterialized lesions
Portal-venous liver perfusion (PLP)	Portal-venous liver blood flow	mL/min/100g of tissue	Detection of predominantly arterialized lesions
Hepatic Perfusion Index (HPI)	ALP/(ALP + PLP)	%	Detection of predominantly arterialized lesions

Table 1. *lists the most commonly used perfusion parameters*

1.8 CONTRAST MEDIUM APPLICATION PRINCIPLES AND SCAN TIMING

Contrast enhancement at CT has been researched in depth over the last decades and a wide range of factors have been discovered to affect contrast enhancement. Those can be divided into three categories: patient-dependent, CT scanning technique-dependent and CM injection-dependent[47-52].

The main patient-dependent factors are body size (weight and height) and cardiac output[47]. Body weight is closely correlated to the patients` blood volume. Bigger patients have a larger blood volume, which results in a dilution of the injected CM and a reduction in iodine concentration in the blood and, consequently, in a lower tissue contrast enhancement. CM volumes should therefore be adjusted for body weight[47].

Cardiac output is the most important factor affecting scan timing. A reduction in cardiac output results in a slower contrast arrival time in the aorta and a delayed peak enhancement in the organ of interest (Figure 9). Differences in contrast arrival time can in part be

overcome with the use of a test-bolus or bolus-tracking technique to individualize the scan timing[47].

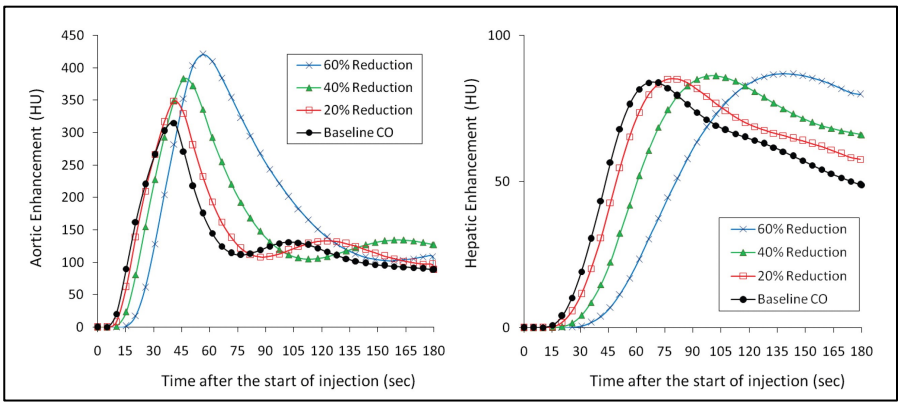

Figure 9. *Simulated contrast enhancement curves of the abdominal aorta (left) and liver (right)based on a hypothetical adult male (30 years old; weight, 70 kg; height, 170 cm) who underwent injection of 125 mL of contrast agent (350 mg of iodine per milliliter) at 4 mL/sec. A set of aortic and hepatic contrast enhancement curves was generated by reducing the baseline cardiac output (CO) by 20%, 40%, and 60%. Reprinted with permission. Radiology, Bae et al[47].*

Other patient-related factors (type of venous access, age, sex, liver cirrhosis, portal hypertension, kidney function and a variety of pathologic conditions) are affecting contrast enhancement to a lesser degree and are therefore not mentioned here in detail.

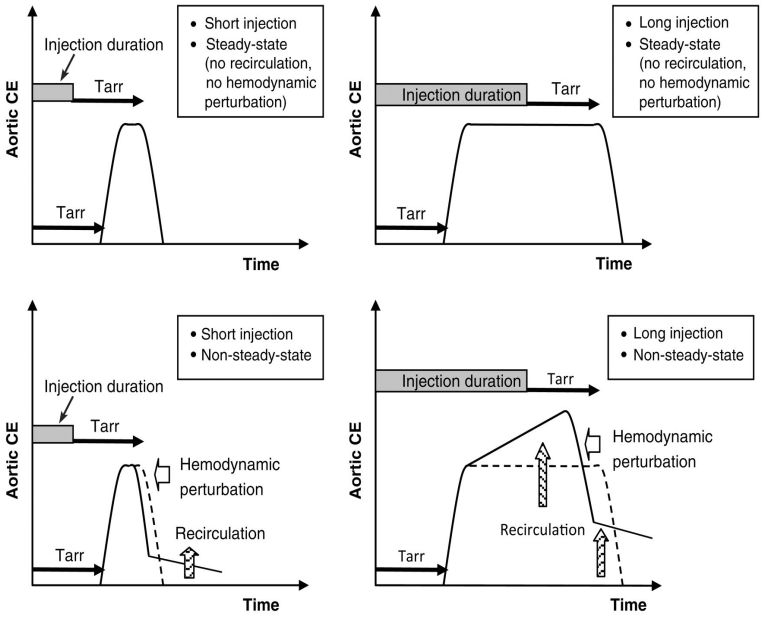

Figure 10. *Time-enhancement curve diagrams illustrate the effect of the injection duration and recirculation on peak contrast enhancement. Top: In a theoretical physiologic model without recirculation or hemodynamic perturbation, aortic contrast enhancement (CE) would show a rapid rise and then a uniform steady-state plateau (a flat broad peak). The time to the end of the plateau enhancement corresponds to the sum of the injection duration plus contrast material arrival time (Tarr) (solid horizontal arrows). Bottom: In reality, however, a fast, large bolus of contrast medium affects and perturbs the hemodynamics of the cardiovascular system, particularly the slow peripheral venous blood flow. This will result in hastening contrast material arrival as the contrast material bolus increases. Because of recirculation (hatched vertical arrows) and hemodynamic perturbation (open horizontal arrows) effect, the steady-state plateau contrast enhancement cannot be sustained and becomes elevated and compressed, resulting in a higher and narrower peak contrast enhancement. The time to peak aortic enhancement becomes shorter than the sum of the injection duration plus contrast material arrival time. Reprinted courtesy to Radiology and Bae KT[47].*

CM-dependent factors are injection duration, injection flow rate, CM concentration, CM volume, bolus shape and whether a saline flush is used or not[47]. For the sake of brevity, only injection duration and CM volume will be discussed here as they are relevant for the understanding of this thesis. The length of the injection duration affects both the extent of enhancement and the scan timing (Figure 10 + 15). A longer injection duration with a constant CM flow rate results in a considerably higher vascular and parenchymal enhancement and a noticeable delay in peak enhancement times[47]. To achieve a desired level of contrast enhancement in the liver in a large group of individuals, a body weight adjusted CM volume should be injected with a fixed injection duration and a constant CM iodine concentration[53-57]. This type of individualized CM protocol facilitates the standardization of scan timing. In other words, the CM volume depends on the patients` weight and the resulting amount of CM then determines the injection flow rate.
Among CT-scanning technique-dependent factors, primarily the scan duration and the chosen scan delay influence the time and height of the peak enhancement (Figure 11)[47]. The bolus-tracking technique is used to determine the CM arrival time and to individualize the scan delay by correcting - to some extent - for cardiac output variations. It is based on sequential monitory scans to depict temporal changes in attenuation within a region of interest (ROI), typically placed in the abdominal aorta for CT imaging of liver. These low dose scans are performed every 1-3 seconds during CM injection until a preset HU threshold is reached[47]. When the threshold is reached, a post-trigger or diagnostic delay is applied.

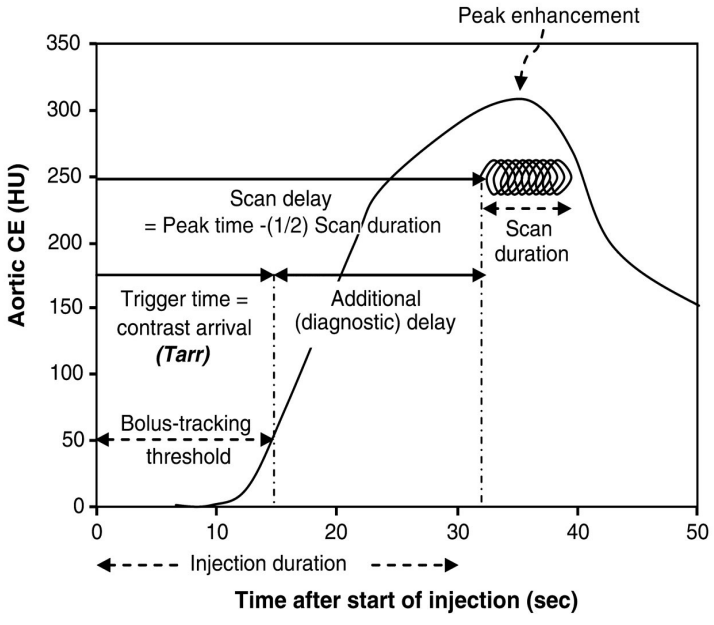

Figure 11. *Graph of contrast medium injection, enhancement, and scan time variables illustrates the determination of scan delay from measured contrast material arrival time (Tarr) and additional diagnostic delay. Scan delay should be determined by considering contrast medium injection duration, contrast material arrival time, and scan duration. Contrast material arrival time can be measured with a test-bolus or bolus-tracking method. In the figure, when bolus-tracking is used, contrast material arrival time corresponds to the time for the aortic enhancement (CE) to reach a 50-HU threshold. The scan delay is determined as the sum of contrast material arrival time plus an additional (diagnostic) delay. The additional diagnostic delay should be formulated considering the injection duration and scan duration such that the peak enhancement is centered in the middle of CT scan (scan delay = peak time – (1/2) scan duration).*
Reprinted courtesy to Radiology and Bae KT[47].

The optimal length of that delay depends on the time to peak enhancement in the target structure and the scan duration, i.e. how long time it takes to image the target volume. The post-trigger delay should equal the time to peak enhancement in the target structure minus half the scan duration (Figure 11). The time to peak enhancement in the target organ is a rather uncertain parameter, influenced by several parameters as described above. There are a number of empiric studies providing information on peak enhancement times in different structures of the body, but these empiric peak enhancement times are only applicable when similar CM injection protocols are used in a comparable study population[47,53-57].

The complexity of contrast enhancement in the human body in general, and in the liver in particular with its dual blood supply, explains the great challenge of optimal CM timing to depict arterially enhancing focal liver lesions.

2 LITERATURE REVIEW: CURRENT APPLICATIONS OF P-CT OF THE LIVER

2.1 DETECTION AND CHARACTERIZATION OF MALIGNANT LIVER TUMORS

Hepatocellular Carcinoma

Hepatocellular carcinoma (HCC) is a highly vascularized tumor and the role of angiogenesis in hepatocarcinogenesis has been well investigated. The change in blood supply from a combined portal venous and arterial to only arterial blood supply due to the development of unpaired arteries and the decrease of intranodal portal supply marks the malignant progression from dysplastic nodule to HCC[12-14]. Therefore, studying the microvasculature of focal liver lesions in comparison to background liver parenchyma has the potential to improve detection and characterization of HCC. Several studies have evaluated perfusion values of HCC and they have all shown significant differences in perfusion values of HCC compared to background cirrhotic liver parenchyma: ALP, HPI, BF, BV and Permeability surface-area product were significantly higher in HCC; whereas PLP, MTT and TTP were lower in HCC as compared to background liver parenchyma[58-62]. Fischer et al. reported an HCC detection rate of 96-98% for side-by-side analysis of color coded perfusion maps (ALP, PLP and HPI) together with time-resolved arterial MIP[63]. To reduce the number of false positive findings a quantitative analysis of HPI with a cut-off value of ≥99 % HPI was recommended, which yielded a specificity of 100% for HCC[63]. The study also demonstrated significantly higher values for ALP and HPI and significantly lower values for PLP when comparing HCC with benign focal liver lesions[63].

Liver metastasis

Several studies have used volume P-CT to investigate the perfusion characteristics of liver metastases of various origins. Perfusion parameters of liver metastases are significantly

different to that of the background liver parenchyma. Goetti et al observed significantly elevated ALP- and HPI-values and significantly lower PLP-values in a collection of 67 metastases of different primary tumors[43]. In a study of Guyennon et al, all investigated CT perfusion parameters were significantly different in hyper-enhancing neuroendocrine liver metastases compared to normal liver parenchyma. BF, BV, PS, ALP and HPI were higher in metastases whereas MTT was shorter than surrounding liver parenchyma[64]. Preliminary results of another study[65] indicated superior detection of colorectal liver metastases on whole liver P-CT compared to standard four-phase CT. Sensitivity increased significantly from 78 % to 89 % and specificity tended to improve slightly, from 78% to 83%. However, the study revealed that P-CT sometimes detects focal benign perfusion changes that can be difficult to distinguish from metastases[65]. In experimental studies on rats, P-CT discovered alterations in liver perfusion when occult liver metastases were present. These results imply that volume P-CT can predict the development of overt liver metastases before they are visible on standard cross-sectional imaging, which could facilitate earlier diagnosis of liver metastases in the future[66].

2.2 HCC-TUMOR GRADING AND PROGNOSIS

A variety of studies have explored if P-CT parameters can be utilized as in vivo biomarkers of neoangiogenesis for different tumor types. For many tumors it has been reported that the grade of tumor vascularization is associated with cancer aggressiveness and that more dense tumor vascularization is correlated with worse clinical outcome. Depicting tumor vascularization might therefore give insights in the prognosis of cancer patients[67].

Goh et al reported that blood volume (BV) and permeability surface-area product correlated positively with histologically evaluated microvessel density in colorectal cancer[67]. Microvessel density is a direct biomarker of angiogenesis but its assessment requires biopsy which is associated with risks of bleeding and of tumor seeding along the biopsy needle path. Chen and colleagues showed that the enhancement pattern on P-CT and the shape of time attenuation curves correlated with microvessel density in HCC[68]. As discussed before, perfusion parameters are significantly changed in HCC, as compared to background liver parenchyma, reflecting HCC tumor microvasculature[58-62]. Nevertheless, there exist contradicting data on P-CTs ability to grade HCC. Sahani et al. discovered significant differences in perfusion parameters (BF, BV and PS) between well differentiated HCC and moderately or poorly differentiated HCC[58]. Ippolito and colleagues, on the other hand, reported no significant association between perfusion values and HCC grade[59].
Zhu et al demonstrated a prognostic value of alterations in MTT pre and post antiangiogenic treatment (bevacizumab) to predict the clinical outcome. They found that a lower baseline value of MTT and a higher percent increase of MTT after bevacizumab was associated with progressive disease in advanced HCC[69].

2.3 ONCOLOGIC THERAPY EVALUATION: LOCO-REGIONAL AND ANTI-ANGIOGENIC TREATMENT

Relatively new treatments such as antiangiogenic drugs or trans-arterial chemoembolization (TACE) target tumor vessel supply. The first tumor response to these treatment forms is not shrinkage but a decrease in tumor vascular supply. This can be difficult to assess with standard imaging methods. With the widespread implementation of these therapies comes the need for new methods that can depict treatment response earlier, before morphologic changes become evident and, furthermore, the need to quantify the response [69-73].

Studies of Zhu et al and Jiang et al demonstrated a significant reduction in BF, BV and PS and a significant increase of MTT 10-12 days after the start of antiangiogenic treatment (bevacizumab)[69,72]. Furthermore, Jiang and colleagues evaluated the performance of P-CT as an imaging biomarker for early treatment response in comparison with the performance of RECIST criteria and measurement of changes in tumor attenuation levels. They discovered that P-CT was a clearly stronger imaging biomarker than the measurement of changes in tumor attenuation, and, furthermore, that RECIST criteria were not reliable for early response evaluation [72].

P-CT has also been successfully used to evaluate early response after TACE[71,74]. In an experimental study on 14 rabbits, TACE-treated areas showed significantly lower values of BF, BV, PS and hepatic arterial fraction and significantly higher values of MTT as compared to pre-treatment perfusion values in implanted VX2-tumors in the liver. Choi et al reported excellent diagnostic performance of P-CT for the detection of recurrent tumor four weeks after TACE; with 100 % sensitivity and specificity, respectively. They found that P-CT values of recurrent tumor were similar to the values of primary tumors before TACE treatment[71].

2.4 DIAGNOSIS AND GRADING OF FIBROSIS AND CIRRHOSIS

The earlier described changes in hepatic circulation in cirrhotic patients can be visualized and quantified with P-CT: P-CT measurements reflect the hepatic arterial buffer response and show a decrease in PLP and total liver perfusion (TLP), as well as a steady increase in ALP and in MTT[5]. Ronot et al. showed that significant changes occur already at intermediate fibrosis[6]. In their study on 52 patients, PLP and TLP were significantly decreased and MTT significantly increased in patients with intermediate fibrosis in comparison to patients with minimal fibrosis.

Hashimoto et al. found a linear relationship between the degree of fibrosis or cirrhosis and an increase in ALP[75].Van Beers and colleagues showed significant correlation between TLP, ALP and MTT and the severity of chronic liver disease[5].

Even though these results are very promising, P-CT can, up to this date, not be used on an individual patient level to securely diagnose or rule out cirrhosis as there is too much individual variation in liver perfusion values. An absolute cut-off value to distinguish

cirrhosis from non-cirrhotic liver disease or healthy liver would, therefore, be problematic to use in clinical routine. Nevertheless, P-CT might in the future play a role in the follow-up of patients with known chronic liver disease to monitor disease progression[5,6].

3 RESEARCH AIMS

General Aims:
To investigate the strengths and limitations of whole liver P-CT and to evaluate if liver P-CT can improve the detection of hyper-vascular liver lesions in patients with chronic liver disease.

Study I: To evaluate if peak splenic enhancement is delayed in patients with portal venous hypertension. To analyze if such a delay would affect the accuracy of perfusion measurements in the liver parenchyma and HCCs using the Dual Maximum Slope Method. Furthermore, to assess if the kidney can replace the spleen to define the separation point of arterial and portal-venous liver perfusion.

Study II: To analyze the variation in HCC peak enhancement times and to design a radiation dose-neutral triple arterial phase protocol from P-CT data. Moreover, to analyze image quality and HCC detection rate in comparison to standard single arterial phase CT.

Study III: To investigate when peak lesion-to-liver contrast (LLC) occurs at high-iodine dose CT imaging and to propose an optimal scan delay for depiction of hyper-vascular liver lesions as well as the hepatic arteries and the portal vein. To compare the performance of a fused radiation dose-neutral quadruple arterial phase CT with standard single arterial phase CT in regard to lesion - and hepatic vessel depiction.

4 MATERIALS AND METHODS

4.1 ETHICAL CONSIDERATIONS

The studies were approved by the local ethical review board in Stockholm, Sweden (registration numbers: 2013/405-31, 2013/1072-32 and 2018/859-31) and by the local committee for radiation protection (registration number: DNR.16/13 and 2018-3132 1792133). Written informed consent was obtained in all studies.

The main ethical concern, when performing studies evaluating volume P-CT, is the relatively high radiation dose used to examine study participants as compared to standard liver CT examinations. Exposure to high levels of ionizing radiation has been shown to increase the risk of radiation induced carcinogenesis[76]. However, this risk is substantially lower in older populations and when effective radiation doses below 100 millisieverts (mSv) are applied[76-78]. Consequently, only older study subjects ($\geq$ 50 years) from a high-risk group of patients were included. The majority of participants (113/132, 86%) had a previous or current malignancy at the time of inclusion. The effective radiation doses applied in our studies ranged from 9.9 mSv to 45 mSv. There is no evidence in the current literature, that effective doses below 100 mSv have the potential to induce new cancer formation[77]. The lag period for developing cancer after exposure to ionizing radiation is a minimum of 5 years and in the majority of cases 10 to 20 years or even longer[76]. In our study population, this would mean that the majority of participants would not live long enough to develop a radiation-induced cancer, both because of their high mean age (68 ± 9 years) at inclusion and also because the majority of participants already had a severely reduced life expectancy due to current/previous cancer. Taking the described factors into account, the risk of ionizing radiation can be seen as acceptable in this thesis` study population.

4.2 STUDY DESIGN

All studies were diagnostic cross-sectional single-center studies. Study I had a retrospective design, whereas Study III was a prospective study. Study II consisted both of a retrospective part for protocol development and a prospective part to assess diagnostic accuracy.

4.3 STUDY POPULATIONS

Study subjects for Study I and II were enrolled from the same patient cohort. Participants were recruited by my co-supervisor and research colleague Michael A. Fischer during his post doc year at Karolinska University Hospital Huddinge in 2013. The study population for Study I and II had an overlap of 11 participants.

Recruitment for Study III was performed by the author of this thesis, and in some cases by my research colleague Anders Svensson-Marcial.
All study subjects were chosen among patients scheduled for a routine multiphasic liver CT because of known or suspected liver malignancy. The inclusion criteria were common for all three studies: Minimum age of at least 50 years, no renal impairment, no known iodine intolerance, and the ability to follow breathing instructions.
The study population of Study I and II consisted in total of 70 patients scanned between March 2012 and September 2014. 7 participants had been scanned with a volume P-CT protocol in a clinical setting and were retrospectively included to the study population after their formal written consent had been obtained.
The 53 participants of Study III were enrolled between September 2018 and February 2020.

4.4 CT PERFUSION IMAGING AND CONTRAST MEDIUM INJECTION PROTOCOLS

All participants were scanned at the same institution (Radiology Department at Karolinska University Hospital Huddinge) on a second generation 128-slice dual-source CT scanner (Siemens SOMATOM Definition Flash, Siemens Healthineers, Forchheim, Germany). Study I and II were performed with identical volume P-CT protocols, but with slightly different low-dose CM injection protocols. Study III was performed with a different P-CT protocol as well as a high iodine dose CM protocol. The amount of CM used in Study III was approximately three-fold higher than the CM volume used in Study I and II. In Study III, the volume P-CT series consisted of 10 scans, while 26-30 scans were obtained in Study I and II. Study III was performed with lower tube current time-product than in the two previous studies (80 or 120 mAs versus 160 or 175 mAs). Furthermore, the scan delay and the cycle time differed between the first two and the third study. The different P-CT Protocols and CM injection protocols are shown in Table 2.

Image Post-Processing:
Automated motion correction and automated 4D noise reduction were performed for all P-CT raw data sets as described in the introduction using a dedicated body perfusion software (Siemens Healthineers, Forchheim, Germany).

Scan Parameters	Perfusion CT Study I & II	Perfusion CT Study III
z coverage, cm	19.2 (14.8–22.1)	21.5 (18.8-25.6)
Scan delay, s	8	5
No. of scans	28 (26–30)	10
Scan direction	cranio-caudal alternating	cranio-caudal alternating
Cycle time, s	1.75	3.5-4.5
Total acquisition time, s	48 (43–54)	35-45
Tube voltage, kV	80	80
Tube current, mAs	160 (-175)	80/120*
Slice collimation, mm	128 x 0.6	128 x 0.6
Gantry rotation time, ms	285	285
Contrast medium injection protocol	**Study I & II**	**Study III**
Volume, ml	50-70	150 (94-188) body-weight adjusted
Iodine concentration, mg/ml	400	400
Flow rate, ml/s	6-7	5.6 (3.7–6.3)
Injection duration, s	8.3-10	25

Table 2. Perfusion CT and Contrast Medium Protocols for Study I-III
**Tube current was 80 mAs in patients weighing <70 kg and 120 mAs in heavier study participants.*

4.5 IMAGE ANALYSIS

Study I:

Twenty-four study subjects were retrospectively chosen from the first study population to form three groups with eight participants each. Participants in Group 1 did not show any imaging based criteria of portal venous hypertension (PVH). Group 2 presented signs of PVH. Group 3 had both imaging based signs of PVH and portal venous thrombosis.
All 24 volume P-CT data sets were uploaded to a post-processing workstation (Multi-Modality Workplace, Siemens Healthineers, Forchheim, Germany) and were further analyzed with a dedicated body perfusion software (Syngo Volume Perfusion CT Body, Siemens Healthineers, Forchheim, Germany). First, time attenuation curves of the spleen and kidney were calculated as shown in Figure 13. The time to, and extent of peak enhancement in those organs were noted. Secondly, the perfusion parameters ALP, PLP

and HPI were calculated for the liver parenchyma and for HCCs using the adapted maximum-slope (AMS) method, first with the spleen and then with the kidney as reference organ, to define the cut-off time point for arterial versus portal venous liver perfusion (Figure 5).

Study II:

The study consisted of two separate parts. First, a group of 15 patients with HCC, who had previously undergone volume P-CT, were retrospectively included to evaluate peak enhancement times in a total of 27 HCC lesions. Peak enhancement times were derived from time attenuation curves, which had been acquired using a dedicated post-processing software ("Dynamic Angio" Application, *Syngo.via*, Siemens Healthineers, Forchheim, Germany). Peak enhancement times were corrected for contrast arrival time variations by subtracting the time until 160 HU was reached in the abdominal aorta. Corrected minimum, mean and maximum HCC peak enhancement times were used as reference to define the timepoints for a dose-neutral time-resolved triple-arterial phase CT (Maximum Intensity Projection) protocol (Figure 12 a).

In the second part, 38 participants were enrolled to undergo both a volume P-CT scan and a standard multiphasic liver CT scan on the same day. Table 3 describes the two different CT and CM protocols. Triple-arterial phase CT images were then created by fusing the split series obtained at the earlier defined three arterial time-points (Figure 12 b). The creation of time-resolved triple-arterial phase images involved also motion-correction and noise-reduction post processing steps, which significantly increase image quality as described in the introduction[46,79,80].

Scan Parameter	Perfusion CT	Standard arterial CT
Z-coverage, cm	19.2 (15.5-22.1)	26.0 (20.1-50.9)
No. of scans	28 (26-30)	1
Total acquisition time, s	48 (43-54)	x
Tube voltage, kV	**80**	**80**
Tube current, mAs	160	automatic tube current modulation
Slice collimation, mm	128 x 0.6	128 x 0.6
Gantry rotation time, ms	285	500
Contrast medium volume, mL	**50**	**120 (70-143) body weight adjusted**
Iodine concentration, mg/mL	400	400
Flow rate, ml/s	6	4.7 (2.9-5.6)
Injection duration, s	8.3	25

Table 3. Overview of the scan protocols of Study II: the volume perfusion CT scan, that was used as a basis for the reconstruction of a time-resolved triple-arterial phase CT and the scan parameters used for the standard single late arterial phase CT.

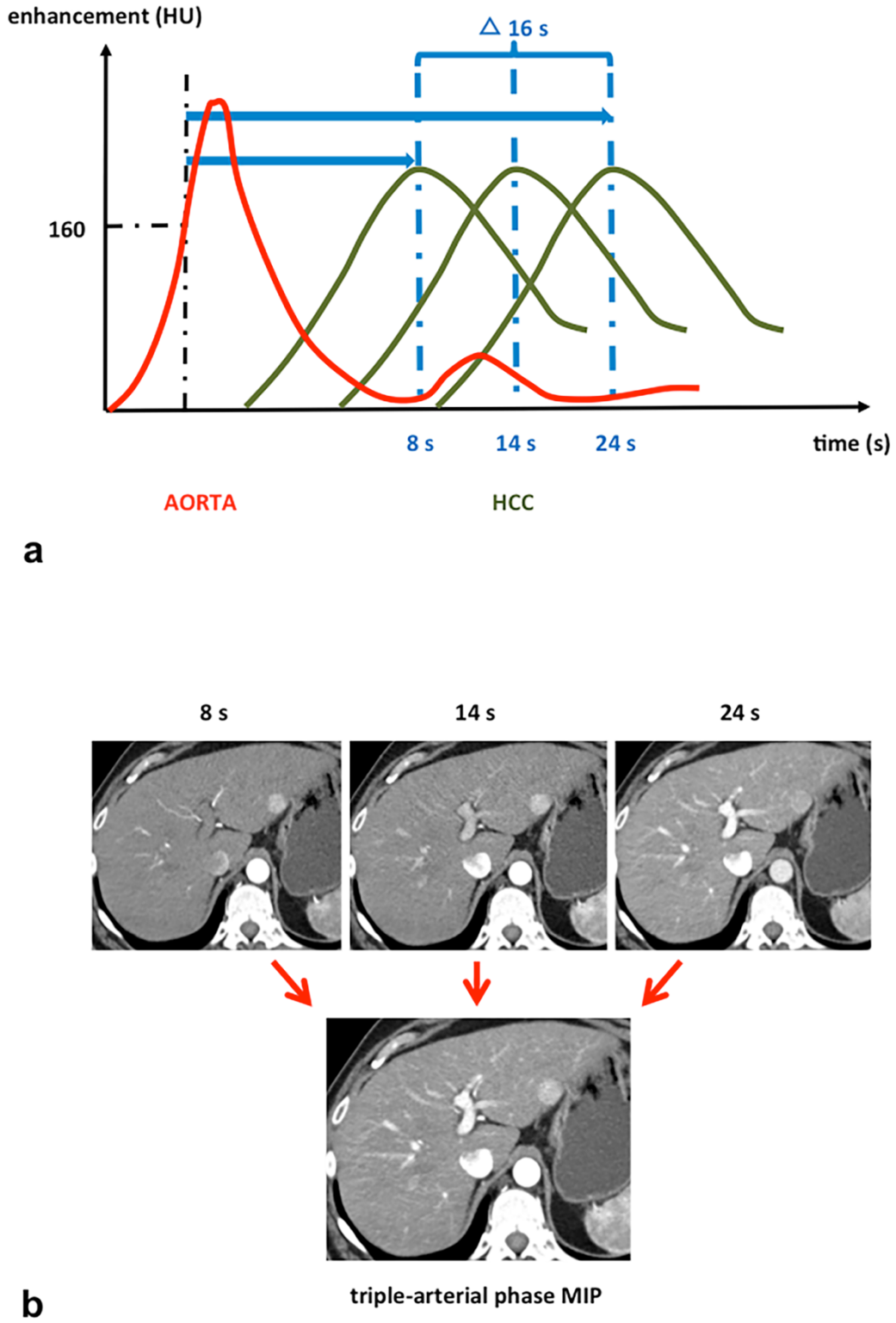

Figure 12. ***a.*** *Illustration of variation of peak enhancement times in 27 HCC lesions from 15 participants in group A. The enhancement curve for the HCC with the minimum (8 s), mean (14 s) and maximum (24 s) time to peak enhancement respectively are shown. The peak enhancement times were corrected for cardiac output variations by subtracting the time until 160 HU was reached in the abdominal aorta. Red curve = aorta. Green curves = HCC lesions. Blue dotted vertical lines mark the peak enhancement in each of the three shown HCC enhancement curves. The black dashed vertical line indicates when 160 HU was reached in the abdominal aorta.*
b. *58-year-old male study participant with a biopsy-proven HCC in liver segment III. These three specific arterial time-points were isolated from the complete perfusion CT data set and fused into a time-resolved triple-arterial phase image set.*

Thus, for each of the 38 study subjects there were two sets of images. One with time-resolved triple-arterial phase CT performed with a bolus of 50 mL CM and one with a standard single arterial phase with a mean CM volume of 120 mL. Both protocols were performed with 80 kV tube voltage. The data sets were evaluated on two separate occasions each by two readers. The performance of triple-arterial phase CT in regards to HCC detection rate, objective and subjective image quality was compared to those of the standard single arterial phase CT. For objective image quality analysis LLC, lesion-to-liver-contrast ratio (LLCR), lesion CNR and image noise were calculated according to the following formulas: number

Lesion-to-liver-contrast (LLC)= mean CT number$_{lesion}$ – mean CT number$_{liver}$

Lesion-to-liver-contrast ratio (LLCR) = (mean CT number$_{lesion}$ – mean CT number$_{liver}$)/ mean CT number$_{liver}$

Contrast-to-noise ratio (CNR) = (mean CT number$_{lesion}$ – mean CT number$_{liver}$)/ SD$_{liver}$

Image Noise = (SD$_{liver}$ + SD$_{air}$)/2

Study III:

53 study subjects were examined with the study specific CT Protocol using a high iodine CM protocol. The CT Protocol consisted of an unenhanced scan, ten arterial volume perfusion scans, a portal venous phase and a delayed phase (Table x).

The study was divided into two separate parts. First, the volume perfusion data sets of 50 participants (Group A) were analyzed using the time attenuation curve function in *Syngo.via* as described above for Study II. Time attenuation curves were created for all detected hyper-vascular liver lesions, the liver parenchyma, the hepatic artery and the portal vein. The time to achieve maximum enhancement difference between each lesion and the surrounding liver parenchyma was noted.

In the second part of the study, all study subjects with hyper-vascular liver lesions were assigned to subgroup A1. For that group, time-resolved quadruple arterial phase image sets were reconstructed after application of motion correction and noise reduction post-processing using the "Dynamic Angio" application in *Syngo.via*. The four time-points were selected according to the results of mean time to peak LLC ± 2 SD. A control group of 16 study participants (Group B) was retrospectively created by systematically searching the picture archiving and communication system (PACS)(IDS7, Sectra AB, Linköping, Sweden). The study subjects of the control group had undergone a standard multiphasic liver CT. It included a standard single arterial phase scan and was obtained during the same time period, using the same scanner as for Group A1 and with an identical CM injection protocol (Table 4).

Phase	Ten-arterial phase perfusion CT scan	Standard single-arterial phase Dual Energy CT scan
Tube Potential, kVp	80	80/140
Tube Current (reference), mAs	80/120*	350/135
Primary Collimation, mm	128 x 0.6	128 x 0.6
Slice Thickness, (Reconstructed/Increment), mm	5.0/2.5	5.0/2.5
Delay, s	+5, 3.5-4.5s interval	+ 20
Gantry Rotation Time, s	0.28	0.5
Acquisitions, number	10	1
Mean z-axis coverage, cm (SD)	21.5 (±2.6)	27.2 (±3.0)
Mean CTDIvol, mGy (SD)	25.7 (±4.4)	9.7 (±2.9)
Mean DLP, mGy (SD)	553.9 (±120.9)	265.4 (±95,1)
Contrast Medium (CM) Protocol		
Body Weight adjusted CM volume, mL	150.1 ± 22.7 (94-188)	149.4 ± 20.7 (124-188)
Iodine concentration, mgI/mL	400	400
CM injection flow rate, ml/s	5.6 ± 0.6 (3.7-6.3)	5.7 ± 0.6 (4.9-7.3)
Injection duration, s	25	25

Table 4. *Scan Parameters and contrast medium injection protocol for Group A (ten arterial phase volume perfusion CT protocol) and Group B (control group performing a standard single arterial phase dual energy protocol.*
**Tube current was 80 mAs in patients weighing <70 kg and 120 mAs in heavier study participants.*

Arterially hyper-enhancing lesions larger than 9 mm in diameter were analyzed for both groups, i.e. for the time-resolved quadruple arterial phase group (A1) and for the standard single arterial phase group (B). Lesion depiction was evaluated by calculating LLC, LLC ratio and lesion CNR as described above for Study II. Moreover, the mean CT number (Hounsfield units, HU) of the hepatic artery and the portal vein as well as the image noise were measured in both groups.

4.6 STATISTICAL ANALYSIS

IBM SPSS (IBM Statistical Package for the Social Sciences Statistics, release 17.0, 24.0 and 28.0; SPSS Inc, Chicago, IL) was used for statistical analysis in all three studies. Quantitative data were descriptively reviewed and tested for normality using the Shapiro-Wilk test or Kolmogorov-Smirnov test. Group comparisons of parametric data were

compared using the independent or paired Student *t* test and analysis of variance (ANOVA), while non-parametric data were analyzed with the Mann-Whitney U test or the Wilcoxon signed rank test. Calculated sensitivities for each reader in Study II were presented with Wilson confidence interval. Confidence ratings (of the Likert Scale) were analyzed using the jackknife alternative free-response receiver operational characteristic (JAFROC) as described by Chakraborty[81]. Performance of triple-arterial phase CT and single-arterial phase were presented as the area under the JAFROC curve (AUC), including 95% confidence intervals (CI). The reliability of the qualitative image evaluation was assessed by the two-way random intraclass correlation coefficient (ICC) of both readers, whereas the interobserver agreement for HCC detection between reader 1 and reader 2 was assessed by Cohen`s Kappa analysis. According to Landis and Koch, a Cohen's kappa coefficient (κ) < 0 is indicating no agreement, 0–0.20 slight, 0.21–0.40 fair, 0.41–0.60 moderate, 0.61–0.80 substantial, and 0.81–1 almost perfect agreement[82]. A p value of < 0.05 was considered statistically significant.

5 RESULTS

5.1 STUDY I

Time to peak renal enhancement (PRE) was similar in all three groups (P=.351). In patients without PVH (Group 1) there was no difference in the time to peak enhancement in the kidney than compared to that in the spleen (P = .247). In patients with PVH (Group 2 and 3) peak splenic enhancement (PSE) was significantly delayed as compared to PRE (P = .03, P = <.001). The time to reach PSE was significantly delayed in patients with portal venous thrombosis (Group 3) compared to Group 1 (without PVH) (P = .012) and Group 2 (P = .004).

Certain perfusion parameters measured in the liver parenchyma were significantly altered in the PVH groups when comparing PSE- and PRE-modelling. For PSE-modelling, PLP was significantly lower and HPI was significantly higher in Group 2 (P = .001; P = .002) as compared to PRE-modelling. ALP was significantly lower in group 3 (P = .043) for PSE-modelling. In Group 3, significantly lower ALP-perfusion values were obtained in HCC lesions with PSE-modeling as compared to PRE-modeling (41.7 ± 9.8 ml/min/100 ml versus 49.0 ± 12.7 ml/min/100 ml, P = .034). In the non-PVH group, there were no significant differences in any of the perfusion parameters measured in the liver or in HCC lesions between PSE- and PRE-modelling.

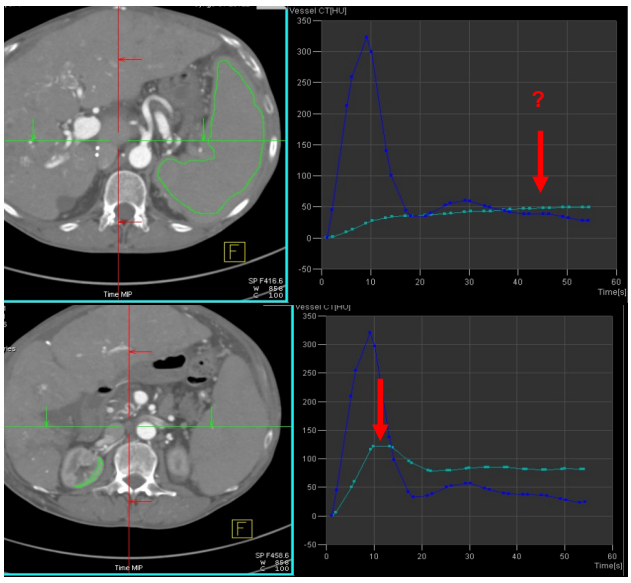

Figure 13. The enhancement curves of kidney and spleen in a 64-year-old male patient with portal venous hypertension and portal vein thrombosis. The splenic enhancement curve (upper right panel) lacks a clear peak and shows delayed enhancement. The renal enhancement curve (in the right lower panel), on the other hand, shows a clear and much earlier peak in the same study subject. The placement of regions of interests in the spleen and kidney (encircled green areas) is shown in the left panels.

5.2 STUDY II

The mean corrected peak enhancement time of the 27 HCC lesions in Group A was 13.4 s with a range of 15.6 s, where the minimum peak enhancement time was 8.1 s and the maximum 23.7 s (Figure 12a).
There was no significant difference in HCC detection rate and overall performance between the triple-arterial phase CT protocol and standard single arterial phase CT (Table 5). Regarding objective image quality, triple-arterial phase CT performed significantly better in lesion CNR (P = .032) and showed significantly less image noise (P < .001) than standard single-arterial CT. Single-arterial phase CT, on the other hand, presented significantly higher LLC (P = .014) and better lesion depiction quality according to both readers (P < .001).

	TP	FP	Sensitivity
Reader 1			
triple-arterial phase	53/65	30	82% [70%, 89%]
single-arterial phase	52/65	39	80% [69%, 88%]
Reader 2			
triple-arterial phase	54/65	20	83% [72%, 90%]
single-arterial phase	50/65	30	77% [65%, 85%]

Overall Performance	**AUC**
triple-arterial phase	0.73 [0.61–0.85]
single-arterial phase	0.60 [0.43–0.77]

Table 5. HCC Detection Rates. Detection rates for reader 1 and 2 using either triple-arterial phase or single-arterial phase CT to detect a total of 65 hepatocellular carcinomas (HCCs) and the overall performance of both protocols. Numbers in brackets are 95% confidence intervals. TP = true positive, FP = false positive, AUC = area under the curve

5.3 STUDY III

There were no statistically significant differences between the two compared groups, ie quadruple arterial phase protocol (Group A1) and standard single arterial CT (Group B), regarding mean age, mean weight, mean length, gender distribution, mean injected CM volume, injection flow rate, mean $CTDI_{vol}$ nor prevalence of liver cirrhosis (Table 6).

	Quadruple arterial phase Group	Single arterial phase Group	p-value
Number of study participants	16	16	1.000
Gender	Female : Male = 1 : 7 (2:14)	Female : Male = 1 : 7 (2:14)	1.000
Age (years)	72 ± 8 (56-84)	72 ± 9 (55-85)	.926
Weight (kg)	85 ± 12 (68-106)	85 ± 17 (66-118)	.724
Length (cm)	174 ± 8 (162-189)	177 ± 10 (156-190)	.210
Body weight adjusted CM dose (mL)	151 ± 17 (124-188)	149 ± 21 (124-188)	.539
CM injection flow rate (ml/s)	5.7 ± 0.4 (4.8-6.3)	5.7 ± 0.6 (4.9-7.3)	1.000
$CTDI_{vol}$ (mGy)	10.5 ± 1.7 (7.5-11.7)	9.7 ± 2.9 (6.3-15.4)	.160
Cirrhosis	14/16 (88 %)	14/16 (88 %)	1.000

Table 6. Demographics (Mean ± Standard Deviations, Range or percentages in parentheses) CM = contrast medium.

The mean time to reach peak LLC after bolus-tracking in the 33 detected hyper-vascular lesions in Group A was 20.1 s (± 4.2s). The inter-lesion variation to achieve peak LLC ranged from 12.5s to 29.1s (Δ16.6s; Table 7). Peak enhancement values and peak enhancement times of the hepatic vascular structures are shown in Table 7.

	TTP LLC (s)	peak LLC (HU)	TTP CHA (s)	TTP portal vein (s)
mean	20.1	124.7	12.7	30.3
SD	4.2	45.1	4.2	4.6
min	12.5	65.0	2.7	20.2
max	29.1	248.0	20.2	43.7

Table 7. Peak enhancement times for hyper-vascular liver lesions, common hepatic artery (CHA) and portal vein in Group A. TTP = time to peak, LLC = lesion-to-liver contrast
Number of lesions total (max. 3 lesions per study participant): 33 lesions in 16/50 (32%) patients
Type of lesion: 30 HCC, 2 iCCC, 1 LiRADs 3-lesion

Both the quadruple arterial phase group (A1) and the standard single arterial phase group (B) contained 33 arterially enhancing lesions each. In Group A1, 30 lesions were defined as HCC according to the diagnostic criteria of AASLD[22], two were biopsy proven intrahepatic cholangiocarcinoma and one was a LiRADs 3-lesion, that had been stable during 2.5 years of follow up. All 33 lesions in Group B were HCC. The evaluation of lesion depiction, image noise and hepatic vessel enhancement showed significantly better results for the quadruple arterial phase group as compared to standard single arterial phase CT: LLC (P = .009), CNR (P=.002) and hepatic artery enhancement (P< .001) were significantly higher and image noise values (P < .001) were significantly lower in the quadruple-arterial phase group. Mean LLCR was 0.9 (± 0.5) for Group A1 and 0.8 (± 0.5) for Group B (P = .139). Mean portal vein enhancement was 287.1 HU (± 75.0 HU) and 266.6 HU (± 81.6 HU) for Group A1 and B, respectively (P = .465).

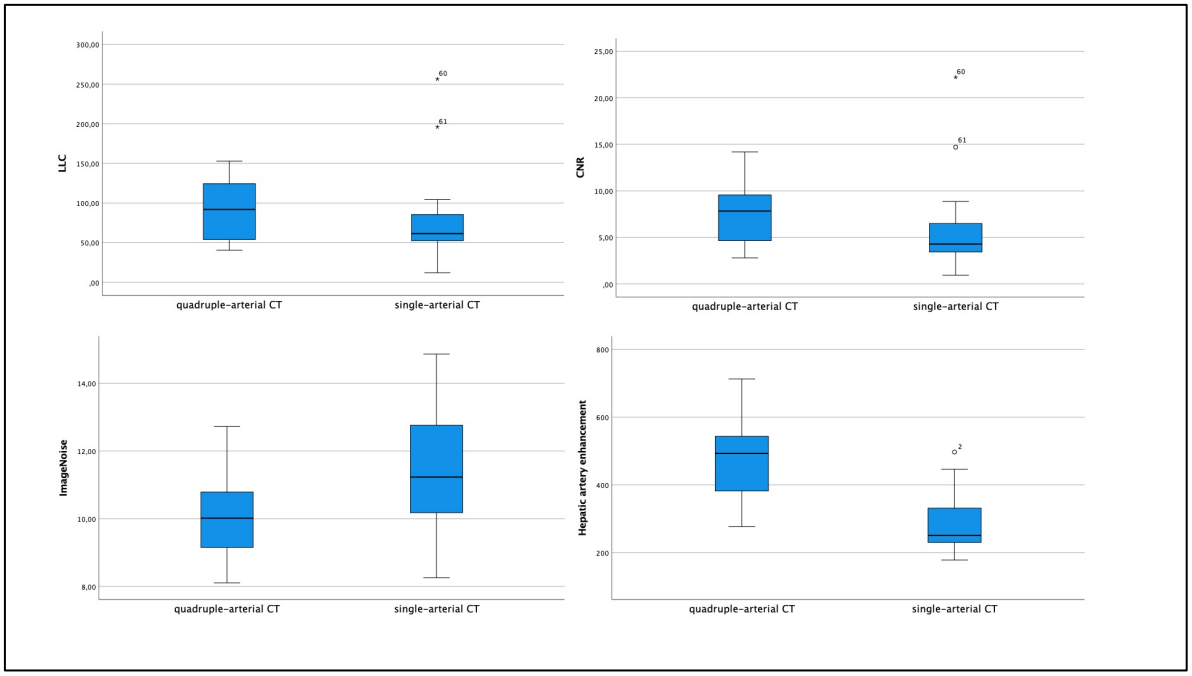

Figure 14. Lesion-to-liver contrast (LLC) and contrast-to-noise ratio (CNR) of the 33 + 33 lesions using quadruple-arterial phase CT and standard single-arterial phase CT, respectively. Image Noise and hepatic artery enhancement in quadruple-arterial phase CT and standard single-arterial phase CT, respectively.

5.4 PATIENT RADIATION EXPOSURE

The radiation dose used for each perfusion split series was higher in the first study population (Study I & II) than that used in Study III, due to a higher tube current-time product. In Study I & II the tube current was set to 160 or 175 mAs. In Study III the tube current was reduced to 80 mAs in patients weighing less than 70 kg and to 120 mAs in heavier study subjects. The reduction in mAs-levels for Study III was an active protocol choice, based on the observed superior objective image quality by triple-arterial phase CT in Study II. Triple-arterial phase CT had, for example, less than half the image noise than that of single arterial phase CT (7.0 ± 2.7 HU versus 15.0 ± 3.0 HU; P < .001). Even with

this 25-55% reduction in mAs-levels for the P-CT protocol of Study III, the image noise was still significantly lower in the time-resolved quadruple arterial phase protocol as compared to the standard single arterial phase protocol (10.0 ± 1.1 HU versus 11.5 ± 1.8 HU; P < .001).

The radiation dose used for the standard late arterial phase protocol was also modified between study II and III. When using the old scan parameters of Study II, three P-CT split series were radiation dose neutral to one standard late arterial phase (3.35 mSv resp. 3.41 mSv; P = .73). In Study III, four split series of the perfusion data set could be used to create a time-resolved quadruple-arterial phase with a similar effective radiation dose as one standard late arterial phase (2.96 mSv resp. 2.79 mSv; P = .160) (Table 8)

	Perfusion CT, single time-point Study I, II / III	**Triple-arterial phase Study II**	**Quadruple-arterial phase Study III**	**Standard late arterial phase Study II / III**
$CTDI_{vol}$ (mGy)	3.88[a] / 2.57[b]	11.64	10.29	11.85[a] / 9.7[b]
DLP (mGycm)	74.5[a] / 49.3[b]	223.3	197.6	227.5[a] / 186.2[b]
Effective dose (mSv)	1.12[a] / 0.74[b]	3.35	2.96	3.41[a] / 2.79[b]

Table 8. The radiation dose required to obtain the arterial phase images for respective protocol in study I-III. The z-coverage was set to 19.2 cm when calculating DLP.
[a] Study I and II. [b] Study III. $CTDI_{vol}$ = CT Dose Index volume, DLP = dose length product
Effective dose was calculated using an abdominal conversion coefficient of 0.015.

6 DISCUSSION

6.1 STUDY I

Main findings:

In patients without portal-venous hypertension (PVH), the peak enhancement of the spleen and kidneys occur almost at the same time. However, in patients with PVH there was a significant delay in the peak enhancement of the spleen. This can be explained by the increased pressure in the portal venous system which might cause venous outflow obstruction and blood pooling in the spleen. The kidneys are not affected by the increased portal-venous pressure, which explains why peak renal enhancement was insensitive to PVH. The slower inflow of CM into the spleen resulted in a flattened splenic enhancement curve in patients with PVH, while the kidney kept its high and clear peak (Figure 13). These observed changes in the splenic enhancement curve in PVH patients affect the calculation of several perfusion parameters of liver parenchyma and hepatocellular carcinomas. In Study I we have proposed a technique to correct this by using the kidney as the reference organ instead of the spleen. We have also shown that it might be possible to quantify PVH by calculating the difference in time to peak enhancement in spleen and kidney.

Discussion and comparison to other research studies:

The Adapted Maximum Slope (AMS) method is a widely used analytical model to calculate liver perfusion since it is mathematically robust, highly reproducible and integrated in commercially available body perfusion software packages. It allows for the calculation of arterial and portal-venous liver perfusion (ALP and PLP), and the proportion of arterial liver perfusion of the total liver perfusion (hepatic perfusion index = HPI)[38,42]. With the AMS method, it is necessary to define the time when peak enhancement in the spleen (PSE) is reached, because this time point is used as a separation point in the calculation of arterial and portal-venous liver perfusion[38,60]. The observations in Study I confirmed our hypothesis that PSE might be delayed in patients with PVH. This was especially true for patient group 3, who had both PVH and portal-venous thrombosis. Similar results were discovered in a later study performed by Talakić et al, who confirmed that using the spleen as a reference organ for the AMS method in patients with PVH is problematic because it alters perfusion measurements in the liver[83]. In the published discussion section in Study I, we stated that "the difference between PSE and PRE might serve as a non-invasive biomarker" to diagnose PVH[84]. Since then, other studies have been performed to evaluate the usefulness of P-CT of the liver and the spleen to assess the presence and severity of PVH in comparison to the reference standard hepatic venous pressure gradient measurements (HVPG)[83,85]. These studies found significant correlation between certain perfusion parameters (splenic clearance, splenic blood volume, K-trans) derived from CT perfusion data of the spleen and conventional invasive HVPG measurements. However, not only P-

CT has shown promising results in this relatively new field but also other non-invasive modalities (transient elastography, MRI elastography and MRI flow gradient measurements) [86-89]. Those latter techniques might be favored as they do not use ionizing radiation.
Nevertheless, the purpose of Study I was primarily to test the hypotheses that peak splenic enhancement times are altered in patients with PVH and that this would affect the calculation of perfusion parameters when using the AMS method. Both hypotheses could be confirmed. In summary, we could offer an alternative way of calculating liver perfusion insensitive to PVH. The proposed method also enables calculation of liver perfusion parameters in patients, who have undergone splenectomy.
An alternative to our method of using the kidney peak enhancement as a reference point, has been proposed by other investigators who instead use the meeting point of the enhancement curves of the aorta and the portal vein[83](Figure 5). Both options seem to work equally well in clinical practice, but have not been compared in a dedicated research study.

Clinical context:
In Study I, a problem that appeared frequently in clinical practice was identified and investigated: The difficulty to use the spleen as a reference organ in CT liver perfusion calculations in patients with PVH when using the AMS method. We could show that the use of peak renal enhancement should be favored in patients with PVH and that these results are directly applicable in clinical practice. Our findings are still relevant up to date, 6 years after their presentation.

Limitations:
Limitations of this study were primarily the small study subject number for each group and the fact that the diagnosis of PVH was imaging based. Ideally, portal venous pressure should have been obtained using the current reference standard of invasive HVPG.

6.2 STUDY II & III

Main findings: Study II showed a great variation in peak enhancement times of HCC lesions and, similarly, Study III demonstrated a comparable variation of time to peak LLC in hyper-vascular liver lesions in cirrhotic patients. We accomplished to create time-resolved triple- respectively quadruple-arterial phase CT images with superior quantitative image quality as compared to standard single arterial phase CT using similar radiation doses as applied in standard single arterial phase CT. The triple-arterial phase protocol in Study II had similar HCC detection rates and equal overall diagnostic performance as standard single arterial phase CT despite the use of less than half of the CM volume. In Study III, an optimal delay for depiction of hyper-vascular liver lesions in cirrhotic patients could be proposed for both single- and multi-arterial phase imaging with a high iodine dose CM protocol.

Discussion and comparison to other research studies:

Selection of the three respectively the four "optimal" time points: In Study II, we retrospectively assessed peak enhancement times of 27 HCC lesions (Group A) to determine the three time points for an optimized time-resolved triple arterial phase CT for detection of arterially enhancing HCCs. The chosen time points referred to the mean time, the shortest and the longest time to reach peak enhancement in those 27 HCCs. The number of time points was chosen to match the radiation dose of a standard single arterial phase CT. Accordingly, in our next study, we could use four time points without increasing the total radiation dose since we had lowered the dose of each split series in the P-CT protocol of Study III. The automated 4D noise reduction software used in both studies analyzes the raw data information of each split series and delivers an incremental improvement in image quality dependent on the number of time points used. Therefore, it was advantageous to use four time points instead of three in Study III, while keeping the total radiation dose constant. The selection process to single out optimal time points for the quadruple phase protocol was improved in Study III, using the experience gained in the previous study. As mentioned earlier, in patients with liver cirrhosis the arterial fraction of liver perfusion increases progressively with the severity of the disease due to the "hepatic arterial buffer response"[4,32]. In severe cirrhosis the arterial enhancement in the liver parenchyma can be so profound that depiction of an HCC lesion at its peak enhancement might coincide with a high enhancement in the surrounding liver tissue. This would result in a lower LLC and a reduction in lesion depiction quality. For Study III, we therefore chose the time to peak LLC as an optimal imaging time point instead of the time of peak HCC enhancement. The four specific time points elected in Study III referred to the two time points closest to the obtained mean time to peak LLC (18s + 22s) as well as plus and minus two SD of this value (12s + 30s). The time to peak LLC was 20.1s (± 4.2s) and since the perfusion split scans were performed with an interval of approximately 4s, the two closest time points to the mean value were 18s and 22s.

Hepatic vessel enhancement in Study III: Hepatic artery enhancement was 1.65 times higher at quadruple arterial phase CT than compared to standard single arterial phase CT. Conventional scan delays to capture a standard single late arterial phase are usually considerably later than the time point of peak enhancement in the hepatic artery. In our study population the peak enhancement time of the hepatic artery was 12.7 s (± 4.2s), while the standard delay for a late arterial phase scan in our institution with the described high iodine dose CM protocol is 20 s. In our quadruple arterial phase protocol, the first selected time point was at 12 s, which more effectively captures hepatic arterial enhancement. This is a big advantage of quadruple-arterial phase CT, since good delineation of hepatic arteries is crucial for therapy planning and tumor staging.

The variation in peak LLC and peak HCC enhancement was similar for both studies and showed a range of 15.6s in Study II and of 16.6s in Study III. Even though both studies applied either "real" or simulated bolus-tracking technique to correct for contrast arrival

time differences in the abdominal aorta, the variation in peak enhancement times was still substantial, reflecting the difficulty of achieving an optimal CM timing with single arterial phase imaging in clinical practice. This problem is commonly known[47] and it has been addressed in the liver imaging community with the proposal to use multi-arterial phase imaging in MRI[90,91]. Previously, dynamic multi-arterial cross-sectional imaging has been reserved to MRI because of the considerable downside of increased radiation dose at multi-arterial phase imaging with CT. Multi-arterial phase imaging at MRI has been shown to improve late arterial phase capture and hyper-vascular lesion detection rate when compared to standard single late arterial phase MRI[90,91].

The novelty of our studies was that we applied a relatively new post-processing technique[46,79,80] to create optimized time-resolved multi-arterial phase CT images with equal radiation dose to that of a standard single late arterial phase scan. This post-processing technique was first described by the authors` co-supervisor Michael A. Fischer[80] who demonstrated significant image quality improvements when several low-dose perfusion split series were fused together after motion correction and automated noise reduction had been applied. These findings were confirmed by Wang et al[79] who also found that fused multi-phasic images had superior quantitative image quality than compared to conventional dual energy single phase CT imaging. Similarly, Study II and III, could also demonstrate significantly enhanced image quality compared to standard single arterial phase imaging despite equal radiation doses applied. Study II revealed significantly higher lesion CNR and significantly lower image noise than at single arterial phase CT. In the same study, LLC and subjective lesion depiction quality were higher in the standard single arterial phase protocol, which can be explained by the more than two-fold higher injected amount of CM. On the other hand in Study III, in which the same CM volumes were given in the quadruple arterial phase group as in the standard single arterial phase group, quadruple arterial phase CT demonstrated significantly higher LLC than standard single arterial phase CT.

The injected CM volume differed considerably between Study II (50 mL) and Study III (150 ± 23 mL), which had several consequences. Injection duration and CM volume both affect the timing and extent of contrast enhancement in different structures. With a longer injection duration and higher administrated contrast volumes, peak enhancement times occur significantly later than when smaller and shorter CM boluses are injected (Figure x)[47]. Consequently, the peak enhancement times derived in Study II could not be copied and transferred to Study III but measurements had to be repeated as described above.

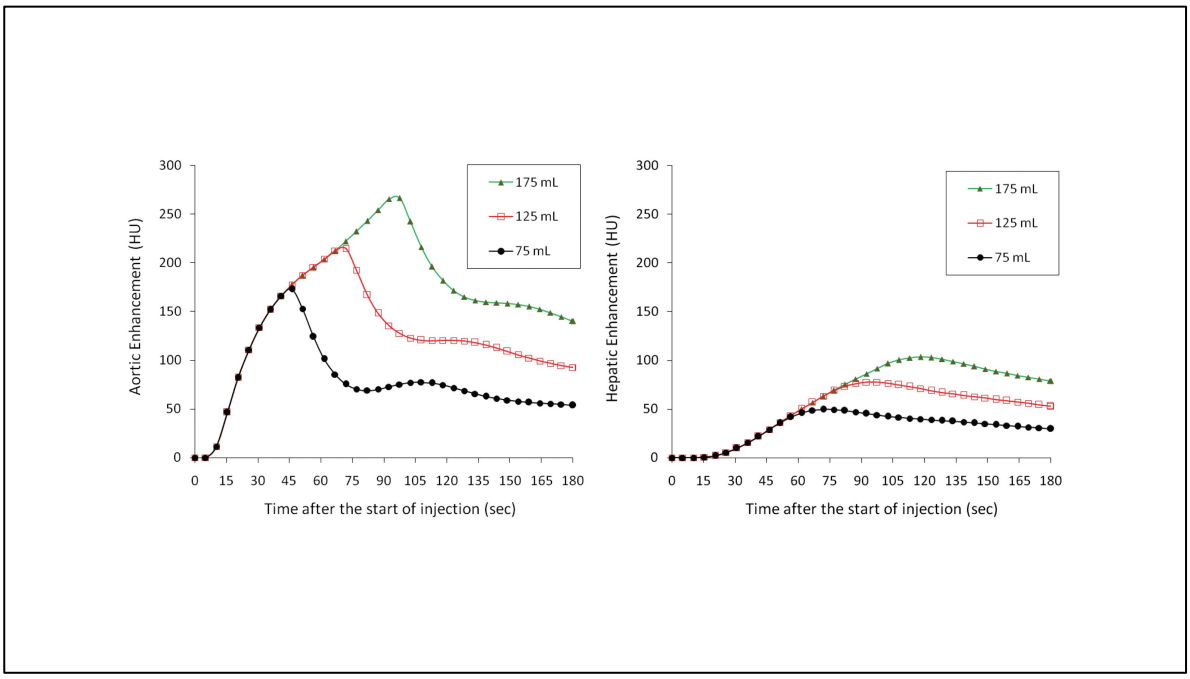

Figure 15. Simulated contrast enhancement curves of the (a) abdominal aorta and (b) liver based on a hypothetical adult male (30 years old; weight, 70 kg; height, 170 cm) subjected to three volumes (75, 125, and 175 mL) of contrast medium (350 mg of iodine per milliliter) injected at the same rate of 2 mL/sec. A larger volume requires a longer duration to inject. Both the time to and the magnitude of the peaks of enhancement increase with the contrast medium volume (injection duration). Reprinted courtesy to Radiology and Bae KT[47].

Study II revealed equal HCC detection rates and similar overall diagnostic performance for triple arterial phase CT with 50 mL administered CM dose as compared to standard single arterial CT with a mean injected dose of 120 mL. This shows that multi-arterial phase CT imaging could be used in patients with impaired kidney function without significant deterioration of diagnostic accuracy. On the other hand, if multi-arterial phase CT imaging is used in combination with a high iodine dose injection protocol, LLC and thus objective lesion depiction quality is significantly augmented as compared to standard single arterial phase imaging performed with the same amount of CM, which might ultimately improve HCC detection.

Study II had some strengths as compared to Study III, and vice versa. The study subjects in Study II were their own control which eliminates certain bias and increases the statistical power when diagnostic accuracy is compared. Moreover, the total number of HCC was almost twice as high as in Study III (65 HCC in Study II versus 33 hyper-enhancing malignant lesions in Study III). The concept of Study III, on the other hand, might be more appealing since we were the first to describe a radiation dose neutral multi-arterial phase CT protocol that can be integrated in a multi-phasic liver CT protocol with standard high iodine dose CM volumes. Furthermore, LLC was significantly higher in the quadruple arterial phase protocol of Study III as compared to standard single arterial phase CT, while it was significantly lower in triple arterial phase CT as compared to standard single arterial phase CT. The improvement of LLC for the quadruple arterial phase CT is a direct effect of the increase in CM volume.

The main limitation of Study III was the low number of patients with hyper-vascular lesions. Accordingly, the study didn`t have enough power to evaluate HCC detection rate in comparison to standard single arterial CT. However, we could show the potential of a tailored quadruple arterial phase protocol for improvement of arterial liver lesion detection and further studies will hopefully follow to underline our findings. In Study II, the standard multiphasic liver CT was, for logistic reasons, acquired approximately 10 minutes after the P-CT, with a risk for residual CM in the standard CT examination. Residual contrast in the liver parenchyma can negatively influence lesion depiction at the standard single arterial phase CT.

Clinical context: Both studies show the added value of multi-arterial phase imaging without increasing the total radiation dose and can be directly implemented in clinical practice. In a clinical scenario in which the CM amount should be minimized due to renal impairment, the multi-arterial phase CT imaging and CM injection protocol of Study II are recommended. In patients with normal kidney function, the CT protocol and CM administration protocol of Study III are favorable because lesion and vessel depiction quality could be further improved with the use of higher amounts of CM and inclusion of a fourth time point. Moreover, even if multi-arterial phase CT imaging might not be possible in another institution due to the use of an older scanner generation or the lack of access to the described post-processing software, our studies still deliver relevant clinical information on optimal diagnostic scan delays at standard single arterial phase CT scans using a high- or a low dose CM protocol.

7 CONCLUSIONS

Study I: Peak splenic enhancement is significantly delayed in patients with portal hypertension, which results in a miscalculation of P-CT parameters. The time to peak renal enhancement is similar for patients with and without portal venous hypertension. Maximum-slope based P-CT could therefore be improved by replacing the spleen with the kidney as the reference organ. The difference between time to peak splenic enhancement and time to peak renal enhancement might serve as a non-invasive biomarker of portal venous hypertension.

Study II: Dose-equivalent triple arterial phase imaging is feasible. Triple arterial phase CT has superior image quality and showed similar HCC detection rate as standard single arterial phase CT even though substantially less CM was administered. Development of a triple arterial phase CT protocol with standard CM dose might improve HCC detection rate.

Study III: When using a high iodine dose CM protocol and bolus-tracking, the optimal scan delay at single arterial phase CT for depiction of hyper-vascular liver lesions occurs at 20 s. Fused quadruple arterial phase CT significantly increases lesion depiction, quantitative image quality and hepatic artery enhancement as compared to standard single arterial phase CT, without elevating the total radiation dose.

8 POINTS OF PERSPECTIVE

Study I: Follow-up studies have been performed by other investigators that both confirm our results and show the usefulness of P-CT of the spleen to evaluate and grade portal venous hypertension[83,85]. However, current investigations also show promising results with other non-invasive modalities, which moreover do not require ionizing radiation and will therefore most likely have more clinical relevance[87]. On the other hand, the usefulness of P-CT to assess the presence or severity of PVH can still be relevant if this information is obtained as a compliment to all the other useful information that P-CT of the upper abdomen delivers.
The main results of Study I are valid up to this date and can be used in clinical practice when evaluating P-CT studies with the AMS model in patients with PVH.

Study II + III: We believe that multi-arterial phase CT imaging has matured to allow for a large scale implementation in clinical practice similar to multi-arterial phase imaging with MRI, which is already state of the art in most liver imaging centers in Europe. The technique can be performed on the majority of CT scanners in use today and the previous limitation of excess radiation dose has now been overcome. The only downside with multi-arterial phase CT imaging as compared to standard single arterial phase CT is the additional time needed to post-process and reconstruct the time-resolved multi-arterial phase images. This can be a problem in high work load or understaffed radiological clinics. Further studies are needed to compare the HCC detection rate between multi-arterial phase imaging and single-arterial phase imaging with a high dose CM protocol. It would also be of interest to evaluate the performance of multi-arterial phase CT regarding its diagnostic performance to detect small HCC lesions (< 2 cm), since these small tumors have a considerable worse detection rate on either standard CT and MRI[28-30]. If these studies show a significant improvement of HCC detection for multi-arterial phase CT imaging, then the multi-arterial phase CT protocol should be implemented and used, to start with, for initial liver tumor staging scans and to assess focal lesions depicted on surveillance ultrasound.

9 ACKNOWLEDGEMENTS

I would like to thank everyone, who contributed to this thesis. Especially, I want to thank:

My principal supervisor **Torkel Brismar** with his unwavering optimism. No obstacle can discourage you. No deadline seems threateningly close. Nothing shakes your positive view on life. In secret, I call you the “Jamaican” because everything you do or say, translates into “Don’t worry, be happy!”. Thank you for your guidance, your record short reply time to correct manuscripts, for taking my night shifts when a research deadline came too close, for pushing me with just the right amount of encouragement. The selection of the main supervisor for one`s PhD thesis is the most important choice during the whole project and I made the right choice with you!

My co-supervisor **Michael Fischer**, who has been the mastermind of this project and delivered most of the ideas and visions behind my thesis. I have learned almost everything I know about Liver Perfusion CT from you! It was a great pleasure to work with you during your post doc year at Karolinska University Hospital Huddinge. Torkel had the most brilliant idea to keep you connected to us by making you my co-supervisor! Thank you for all your professional guidance, many fruitful discussions during the study design processes and endless email correspondence during manuscript writing!

My co-supervisor **Per Stål** for his incredible knowledge in hepatology, his kindness and patience as well as his genuine interest in my research. Thank you for being there whenever I needed you!

My first research department professor **Peter Aspelin** for creating the best possible research climate at our department and teaching Torkel to keep your legacy alive! There is not one person in our clinic, who has not been inspired by you and the majority of my research colleagues started research because of you! It is an honor to know you and to have picked your brain on a few occasions!

My colleague and co-author **Anders Svensson-Marcial** for his research enthusiasm and fast implementation of theories and ideas into real life projects. Thank you for recruiting and scanning the vast majority of patients for me! Without you, I would still be looking for patients to enroll for my studies. Your exceptional skills in CT imaging are inspiring. Thank you for generously sharing your CT knowledge with me!

My CT- and emergency radiology mentor **Bertil Leidner**, who together with Michael Fischer introduced me to Liver Perfusion CT. You have been a real role model for me with your never-ending quest to improve CT protocols and emergency radiology work flows. Thank you for generously sharing so much of your CT knowledge and diagnostic skills with me and so many other former residents!

My clinical supervisors during my residency at Karolinska University Hospital Huddinge and fellow German speakers **Susanne Müller**, **Christine** and **Klaus Lange**. Thank you for your intimate guidance and support inside and outside of the Radiology Department! You have become like family to me!

ALL my fantastic colleagues from the **abdominal radiology section** during all my years at Karolinska Huddinge. I have learned everything I know from you! Thank you for working clinical cases when I had research leave and for inspiring me to become a more skilled radiologist!

My amazing colleagues from the **thoracic radiology section** at Karolinska Huddinge, especially Laura Saiepour, Ulrika Håkansson, Raquel Themudo and Louise Norlén for supporting me and my research.

Thank you to all my former bosses **Elisabet Axelsson, Natalia Luotsinen and Jan Carlson,** who have supported my research and cleared my schedule so that I could accomplish this thesis.

My friend, boss and colleague **Louiza Loizou** for creating the best work environment one could hope for! I hope you will be our boss forever!

My fellow PhD colleagues **Antonios Tzortzakakis, Johan Teiler** and **Yngve Forslin** who have helped and supported me both morally and with many practical tips.

My friend and absolutely genius PhD colleague **Sara Shams**, who helped me organize a short visiting internship at Stanford Hospital and Stanford University School of Medicine. She was kind enough to open her home to me and to introduce me to all her brilliant teachers and consultants.

The former and current **CT staff**, both radiographers and all nurses from the patient scheduling office. You have taught me a lot and helped me so much to recruit the patients for this thesis!

Min fina granne **Heléne** som hoppade in som barnvakt och extra-mormor otaliga gånger med kort varsel. Du är världens finaste person och vi är så glada att vi har dig i vårt liv! Utan dig hade jag aldrig haft möjligheten att skriva klart min avhandling! Stort tack!

All personal på förskolan ”Väktaren”, fram för allt **Fairouz**, **Sara** och **Kicki** som tar så bra hand om min son. Ert fantastiska engagemang gör vardagen så mycket lättare och det uppskattar jag jättemycket!

My early role models, **Juliane** and **Sylvia**. You have inspired me with your sharp clinical skills and your fierce position in the men-dominated hospital world. I chose my profession because of you!

A mi familia española, **María, Pablo grande, Carmen** y **Gregorio**. Gracias por acogerme como a vuestra tercera hija y por vuestro apoyo y cariño incondicional.

My family. My parents **Ursula** and **Reinhard** for always prioritizing and supporting my education and my happiness, and for teaching me the right values in life. My dear sister and fellow PhD **Babsi** for leading the way and showing me that writing a PhD thesis with a small child at home is possible. I love you all very much!

My adorable son **Pablo**, who did everything in his mighty power to distract me from writing this thesis. Thank you for your unconditional love and all the joy you give to me! You and Laura put everything into perspective and show me what is really important in my life!

Most importantly, my person. My beautiful and brilliant partner in life, **Laura**, who literally kept me alive while writing this thesis. Your curious mind is always working overtime and it has inspired me many times to grow with you. Thank you for your never ending support and your patience. I know that this was a very hard time for all of us and I`m really looking forward to more relaxing and joyful times! You are the best partner and co-mama I could ask for! I love you so much! Té amo!

10 REFERENCES

1. Elias H, Petty D. Gross anatomy of the blood vessels and ducts within the human liver. *Am J Anat.* 1952;90(1):59-111.
2. Kiernan F, Green, J. H. The anatomy and physiology of the liver. . *Philosophical Transactions of the Royal Society of London.* 1837;3:211-212.
3. Segmental anatomy of the liver. Accessed 2022/04/05.
4. Eipel C, Abshagen K, Vollmar B. Regulation of hepatic blood flow: The hepatic arterial buffer response revisited. *World Journal of Gastroenterology : WJG.* 2010;16(48):6046-6057.
5. Van Beers BE, Leconte I, Materne R, Smith AM, Jamart J, Horsmans Y. Hepatic perfusion parameters in chronic liver disease: dynamic CT measurements correlated with disease severity. *AJR Am J Roentgenol.* 2001;176(3):667-673.
6. Ronot M, Asselah T, Paradis V, et al. Liver Fibrosis in Chronic Hepatitis C Virus Infection: Differentiating Minimal from Intermediate Fibrosis with Perfusion CT. *Radiology.* 2010;256(1):135-142.
7. Sung H, Ferlay J, Siegel RL, et al. Global Cancer Statistics 2020: GLOBOCAN Estimates of Incidence and Mortality Worldwide for 36 Cancers in 185 Countries. *CA: A Cancer Journal for Clinicians.* 2021;71(3):209-249.
8. McGlynn KA, Petrick JL, El-Serag HB. Epidemiology of Hepatocellular Carcinoma. *Hepatology.* 2021;73(S1):4-13.
9. Brunt E, Aishima S, Clavien PA, et al. cHCC-CCA: Consensus terminology for primary liver carcinomas with both hepatocytic and cholangiocytic differentation. *Hepatology.* 2018;68(1):113-126.
10. Miles KA, Lee TY, Goh V, et al. Current status and guidelines for the assessment of tumour vascular support with dynamic contrast-enhanced computed tomography. *European Radiology.* 2012;22(7):1430-1441.
11. Miles KA. Tumour angiogenesis and its relation to contrast enhancement on computed tomography: a review. *European Journal of Radiology.* 1999;30(3):198-205.
12. Muto J, Shirabe K, Sugimachi K, Maehara Y. Review of angiogenesis in hepatocellular carcinoma. *Hepatol Res.* 2015;45(1):1-9.
13. Kitao A, Zen Y, Matsui O, Gabata T, Nakanuma Y. Hepatocarcinogenesis: Multistep Changes of Drainage Vessels at CT during Arterial Portography and Hepatic Arteriography—Radiologic-Pathologic Correlation. *Radiology.* 2009;252(2):605-614.
14. Matsui O, Kobayashi S, Sanada J, et al. Hepatocelluar nodules in liver cirrhosis: hemodynamic evaluation (angiography-assisted CT) with special reference to multi-step hepatocarcinogenesis. *Abdominal Imaging.* 2011;36(3):264-272.
15. Llovet JM, Kelley RK, Villanueva A, et al. Hepatocellular carcinoma. *Nature Reviews Disease Primers.* 2021;7(1):6.

16. EASL Clinical Practice Guidelines: Management of hepatocellular carcinoma. *J Hepatol.* 2018;69(1):182-236.

17. Kew MC. Synergistic interaction between aflatoxin B1 and hepatitis B virus in hepatocarcinogenesis. *Liver International.* 2003;23(6):405-409.

18. Global Burden of Disease Liver Cancer C. The Burden of Primary Liver Cancer and Underlying Etiologies From 1990 to 2015 at the Global, Regional, and National Level: Results From the Global Burden of Disease Study 2015. *JAMA Oncology.* 2017;3(12):1683-1691.

19. Bruix J, Llovet JM. Prognostic prediction and treatment strategy in hepatocellular carcinoma. *Hepatology.* 2002;35(3):519-524.

20. Marrero JA, Fontana RJ, Barrat A, et al. Prognosis of hepatocellular carcinoma : Comparison of 7 staging systems in an American cohort. *Hepatology (Baltimore, Md).* 2005;41(4):707-716.

21. Llovet JM, Brú C, Bruix J. Prognosis of hepatocellular carcinoma: the BCLC staging classification. *Seminars in liver disease.* 1999;19(3):329-338.

22. Marrero JA, Kulik LM, Sirlin CB, et al. Diagnosis, Staging, and Management of Hepatocellular Carcinoma: 2018 Practice Guidance by the American Association for the Study of Liver Diseases. *Hepatology.* 2018;68(2):723-750.

23. Bolondi L. Screening for hepatocellular carcinoma in cirrhosis. *Journal of Hepatology.* 2003;39(6):1076-1084.

24. Bruix J, Sherman M, Llovet JM, et al. Clinical Management of Hepatocellular Carcinoma. Conclusions of the Barcelona-2000 EASL Conference. *Journal of Hepatology.* 2001;35(3):421-430.

25. Chernyak V, Fowler KJ, Kamaya A, et al. Liver Imaging Reporting and Data System (LI-RADS) Version 2018: Imaging of Hepatocellular Carcinoma in At-Risk Patients. *Radiology.* 2018;289(3):816-830.

26. Fowler KJ, Hecht E, Kielar AZ, Singal AG, Sirlin CB. LI-RADS v2018: a Primer and Update for Clinicians. *Current Hepatology Reports.* 2018;17(4):425-433.

27. Lee YJ, Lee JM, Lee JS, et al. Hepatocellular Carcinoma: Diagnostic Performance of Multidetector CT and MR Imaging—A Systematic Review and Meta-Analysis. *Radiology.* 2015;275(1):97-109.

28. Forner A, Vilana R, Ayuso C, et al. Diagnosis of hepatic nodules 20 mm or smaller in cirrhosis: Prospective validation of the noninvasive diagnostic criteria for hepatocellular carcinoma. *Hepatology.* 2008;47(1):97-104.

29. Lauenstein TC, Salman K, Morreira R, et al. Gadolinium-enhanced MRI for tumor surveillance before liver transplantation: center-based experience. *AJR Am J Roentgenol.* 2007;189(3):663-670.

30. Luca A, Caruso S, Milazzo M, et al. Multidetector-row computed tomography (MDCT) for the diagnosis of hepatocellular carcinoma in cirrhotic candidates for liver transplantation: prevalence of radiological vascular patterns and histological correlation with liver explants. *Eur Radiol.* 2010;20(4):898-907.

31. Kartalis N, Brehmer K, Loizou L. Multi-detector CT: Liver protocol and recent developments. *Eur J Radiol.* 2017;97:101-109.

32. Kim SH, Kamaya A, Willmann JK. CT perfusion of the liver: principles and applications in oncology. *Radiology.* 2014;272(2):322-344.

33. Kambadakone AR, Sahani DV. Body Perfusion CT: Technique, Clinical Applications, and Advances. *Radiologic Clinics of North America.* 2009;47(1):161-178.

34. Blomley MJ, Coulden R, Dawson P, et al. Liver perfusion studied with ultrafast CT. *J Comput Assist Tomogr.* 1995;19(3):424-433.

35. Cuenod CA, Balvay D. Perfusion and vascular permeability: Basic concepts and measurement in DCE-CT and DCE-MRI. *Diagnostic and Interventional Imaging.* 2013;94(12):1187-1204.

36. Miles KA. Measurement of tissue perfusion by dynamic computed tomography. *The British journal of radiology.* 1991;64(761):409-412.

37. Miles KA. Functional computed tomography in oncology. *European Journal of Cancer.* 2002;38(16):2079-2084.

38. Miles KA, Hayball MP, Dixon AK. Functional images of hepatic perfusion obtained with dynamic CT. *Radiology.* 1993;188(2):405-411.

39. Patlak CS, Blasberg RG, Fenstermacher JD. Graphical evaluation of blood-to-brain transfer constants from multiple-time uptake data. *Journal of cerebral blood flow and metabolism : official journal of the International Society of Cerebral Blood Flow and Metabolism.* 1983;3(1):1-7.

40. Johnson JA, Wilson TA. A model for capillary exchange. *The American journal of physiology.* 1966;210(6):1299-1303.

41. Miles KA, Charnsangavej C, Lee FT, Fishman EK, Horton K, Lee T-Y. Application of CT in the investigation of angiogenesis in oncology. *Academic Radiology.* 2000;7(10):840-850.

42. Tsushima Y, Funabasama S, Aoki J, Sanada S, Endo K. Quantitative perfusion map of malignant liver tumors, created from dynamic computed tomography data. *Acad Radiol.* 2004;11(2):215-223.

43. Goetti R, Leschka S, Desbiolles L, et al. Quantitative computed tomography liver perfusion imaging using dynamic spiral scanning with variable pitch: feasibility and initial results in patients with cancer metastases. *Invest Radiol.* 2010;45(7):419-426.

44. DV S. Perfusion CT: An Overview Of Technique And Clinical Applications. 2010.

45. Klotz E, Haberland U, Glatting G, et al. Technical prerequisites and imaging protocols for CT perfusion imaging in oncology. *European Journal of Radiology.* 2015;84(12):2359-2367.

46. Wang H, Krishnan S, Wang X, et al. Improving soft-tissue contrast in four-dimensional computed tomography images of liver cancer patients using a deformable image registration method. *International journal of radiation oncology, biology, physics.* 2008;72(1):201-209.

47. Bae KT. Intravenous Contrast Medium Administration and Scan Timing at CT: Considerations and Approaches. *Radiology.* 2010;256(1):32-61.

48. Kondo H, Kanematsu M, Goshima S, et al. MDCT of the pancreas: optimizing scanning delay with a bolus-tracking technique for pancreatic, peripancreatic

vascular, and hepatic contrast enhancement. *AJR Am J Roentgenol.* 2007;188(3):751-756.

49. Goshima S, Kanematsu M, Moriyama N, et al. Pancreas : Optimal scan delay for contrast-enhanced multi-detector row CT. *Radiology.* 2006;241(1):167-174.

50. Bae KT, Heiken JP. Scan and contrast administration principles of MDCT. *European Radiology Supplements.* 2005;15(S5):e46-e59.

51. Fleischmann D, Kamaya A. Optimal vascular and parenchymal contrast enhancement: the current state of the art. *Radiol Clin North Am.* 2009;47(1):13-26.

52. Heiken JP, Brink JA, McClennan BL, Sagel SS, Crowe TM, Gaines MV. Dynamic incremental CT: effect of volume and concentration of contrast material and patient weight on hepatic enhancement. *Radiology.* 1995;195(2):353-357.

53. Goshima S, Kanematsu M, Kondo H, et al. MDCT of the liver and hypervascular hepatocellular carcinomas: optimizing scan delays for bolus-tracking techniques of hepatic arterial and portal venous phases. *AJR Am J Roentgenol.* 2006;187(1):W25-32.

54. Kagawa Y, Okada M, Yagyu Y, et al. Optimal scan timing of hepatic arterial-phase imaging of hypervascular hepatocellular carcinoma determined by multiphasic fast CT imaging technique. *Acta radiologica (1987).* 2013;54(8):843-850.

55. Kanematsu M, Goshima S, Kondo H, et al. Optimizing scan delays of fixed duration contrast injection in contrast-enhanced biphasic multidetector-row CT for the liver and the detection of hypervascular hepatocellular carcinoma. *Journal of computer assisted tomography.* 2005;29(2):195-201.

56. Murakami T, Kim T, Kudo M, et al. Hypervascular hepatocellular carcinoma : Detection with double arterial phase multi-detector row helical CT. *Radiology.* 2001;218(3):763-767.

57. Sultana S, Awai K, Nakayama Y, et al. Hypervascular hepatocellular carcinomas : Bolus tracking with a 40-detector CT scanner to time arterial phase imaging. *Radiology.* 2007;243(1):140-147.

58. Sahani DV, Holalkere N-S, Mueller PR, Zhu AX. Advanced Hepatocellular Carcinoma: CT Perfusion of Liver and Tumor Tissue—Initial Experience. *Radiology.* 2007;243(3):736-743.

59. Ippolito D, Capraro C, Casiraghi A, Cestari C, Sironi S. Quantitative assessment of tumour associated neovascularisation in patients with liver cirrhosis and hepatocellular carcinoma: role of dynamic-CT perfusion imaging. *European Radiology.* 2011;22(4):803-811.

60. Kaufmann S, Horger T, Oelker A, et al. Characterization of hepatocellular carcinoma (HCC) lesions using a novel CT-based volume perfusion (VPCT) technique. *European Journal of Radiology.* 2015;84(6):1029-1035.

61. Ippolito D, Sironi S, Pozzi M, et al. Hepatocellular Carcinoma in Cirrhotic Liver Disease: Functional Computed Tomography With Perfusion Imaging in the Assessment of Tumor Vascularization. *Academic Radiology.* 2008;15(7):919-927.

62. Ippolito D, Sironi S, Pozzi M, et al. Perfusion CT in cirrhotic patients with early stage hepatocellular carcinoma: Assessment of tumor-related vascularization. *European Journal of Radiology.* 2010;73(1):148-152.

63. Fischer MA, Kartalis N, Grigoriadis A, et al. Perfusion computed tomography for detection of hepatocellular carcinoma in patients with liver cirrhosis. *Eur Radiol.* 2015;25(11):3123-3132.

64. Guyennon A, Mihaila M, Palma J, Lombard-Bohas C, Chayvialle JA, Pilleul F. Perfusion characterization of liver metastases from endocrine tumors: Computed tomography perfusion. *World journal of radiology.* 2010;2(11):449-454.

65. Meijerink MR, van Waesberghe JH, van der Weide L, van den Tol P, Meijer S, van Kuijk C. Total-liver-volume perfusion CT using 3-D image fusion to improve detection and characterization of liver metastases. *Eur Radiol.* 2008;18(10):2345-2354.

66. Cuenod C, Leconte I, Siauve N, et al. Early changes in liver perfusion caused by occult metastases in rats: detection with quantitative CT. *Radiology.* 2001;218(2):556-561.

67. García-Figueiras R, Goh VJ, Padhani AR, et al. CT Perfusion in Oncologic Imaging: A Useful Tool? *American Journal of Roentgenology.* 2013;200(1):8-19.

68. Chen W-X, Min P-Q, Song B, Xiao B-L, Liu Y, Ge Y-H. Single-level dynamic spiral CT of hepatocellular carcinoma: Correlation between imaging features and density of tumor microvessels. *World Journal of Gastroenterology.* 2004;10(1):67-72.

69. Zhu AX, Holalkere NS, Muzikansky A, Horgan K, Sahani DV. Early Antiangiogenic Activity of Bevacizumab Evaluated by Computed Tomography Perfusion Scan in Patients with Advanced Hepatocellular Carcinoma. *The Oncologist.* 2008;13(2):120-125.

70. Chen G, Ma D-Q, He W, Zhang B-F, Zhao L-Q. Computed tomography perfusion in evaluating the therapeutic effect of transarterial chemoembolization for hepatocellular carcinoma. *World Journal of Gastroenterology : WJG.* 2008;14(37):5738-5743.

71. Choi SH, Chung JW, Kim HC, et al. The role of perfusion CT as a follow-up modality after transcatheter arterial chemoembolization: an experimental study in a rabbit model. *Invest Radiol.* 2010;45(7):427-436.

72. Jiang T, Kambadakone A, Kulkarni NM, Zhu AX, Sahani DV. Monitoring response to antiangiogenic treatment and predicting outcomes in advanced hepatocellular carcinoma using image biomarkers, CT perfusion, tumor density, and tumor size (RECIST). *Invest Radiol.* 2012;47(1):11-17.

73. Jiang T, Zhu AX, Sahani DV. Established and novel imaging biomarkers for assessing response to therapy in hepatocellular carcinoma. *Journal of Hepatology.* 2013;58(1):169-177.

74. Marquez HP, Karalli A, Haubenreisser H, et al. Computed tomography perfusion imaging for monitoring transarterial chemoembolization of hepatocellular carcinoma. *Eur J Radiol.* 2017;91:160-167.

75. Hashimoto K, Murakami T, Dono K, et al. Assessment of the severity of liver disease and fibrotic change: the usefulness of hepatic CT perfusion imaging. *Oncology reports.* 2006;16(4):677-683.

76. Lin EC. Radiation risk from medical imaging. *Mayo Clin Proc.* 2010;85(12):1142-1146; quiz 1146.

77. Hendee WR, O'Connor MK. Radiation Risks of Medical Imaging: Separating Fact from Fantasy. *Radiology.* 2012;264(2):312-321.

78. Verdun FR, Bochud F, Gundinchet F, Aroua A, Schnyder P, Meuli R. Quality Initiatives Radiation Risk: What You Should Know to Tell Your Patient. *RadioGraphics.* 2008;28(7):1807-1816.

79. Wang X, Henzler T, Gawlitza J, et al. Image quality of mean temporal arterial and mean temporal portal venous phase images calculated from low dose dynamic volume perfusion CT datasets in patients with hepatocellular carcinoma and pancreatic cancer. *European Journal of Radiology.* 2016;85(11):2104-2110.

80. Fischer MA, Leidner B, Kartalis N, et al. Time-resolved computed tomography of the liver: retrospective, multi-phase image reconstruction derived from volumetric perfusion imaging. *Eur Radiol.* 2014;24(1):151-161.

81. Chakraborty DP. Analysis of location specific observer performance data: validated extensions of the jackknife free-response (JAFROC) method. *Acad Radiol.* 2006;13(10):1187-1193.

82. Landis JR, Koch GG. The measurement of observer agreement for categorical data. *Biometrics.* 1977;33(1):159-174.

83. Talakić E, Schaffellner S, Kniepeiss D, et al. CT perfusion imaging of the liver and the spleen in patients with cirrhosis: Is there a correlation between perfusion and portal venous hypertension? *Eur Radiol.* 2017;27(10):4173-4180.

84. Fischer MA, Brehmer K, Svensson A, Aspelin P, Brismar TB. Renal versus splenic maximum slope based perfusion CT modelling in patients with portal-hypertension. *Eur Radiol.* 2016.

85. Tsushima Y, Koizumi J, Yokoyama H, Takeda A, Kusano S. Evaluation of portal pressure by splenic perfusion measurement using dynamic CT. *AJR Am J Roentgenol.* 1998;170(1):153-155.

86. Gouya H, Grabar S, Vignaux O, et al. Portal hypertension in patients with cirrhosis: indirect assessment of hepatic venous pressure gradient by measuring azygos flow with 2D-cine phase-contrast magnetic resonance imaging. *European radiology.* 2015;26(7):1981-1990.

87. Kennedy P, Bane O, Hectors SJ, et al. Noninvasive imaging assessment of portal hypertension. *Abdominal radiology (New York).* 2020;45(11):3473-3495.

88. Wagner M, Hectors S, Bane O, et al. Noninvasive prediction of portal pressure with MR elastography and DCE-MRI of the liver and spleen: Preliminary results. *Journal of magnetic resonance imaging.* 2018;48(4):1091-1103.

89. Ronot M, Lambert S, Elkrief L, et al. Assessment of portal hypertension and high-risk oesophageal varices with liver and spleen three-dimensional multifrequency MR elastography in liver cirrhosis. *European radiology.* 2014;24(6):1394-1402.

90. Clarke SE, Saranathan M, Rettmann DW, Hargreaves BA, Vasanawala SS. High resolution multi-arterial phase MRI improves lesion contrast in chronic liver disease. *2015.* 2015:10.

91. Kazmierczak PM, Theisen D, Thierfelder KM, et al. Improved detection of hypervascular liver lesions with CAIPIRINHA-Dixon-TWIST-volume-interpolated breath-hold examination. *Invest Radiol.* 2015;50(3):153-160.